Tropospheric Ozone Production Pathways with Detailed Chemical Mechanisms

Dissertation zur Erlangung des akademischen Grades
des Doktors der Naturwissenschaftern
am Fachbereich Geowissenschaften
an der Freien Universität Berlin

Vorgelegt von
Jane Coates
im Juli 2016

1. Gutachter: Prof. Dr. Peter Builtjes
2. Gutachter: Prof. Dr. Mark Lawrence

Acknowledgements

Table of Contents

List of Tables

List of Figures

Chapter 1

Introduction

Air pollution is the leading environmental health risk in many areas around the world. The effects of air pollution to the general population range from chronic to less severe health impacts and reduced growth rates of vegetation resulting in economic losses of billions of euros (EEA, 2015). Moreover, the International Agency for Research on Cancer labelled air pollution as carcinogenic (IARC, 2013). Due to these impacts, many governed areas introduced legislation designed to reduce concentrations of many air pollutants.

Tropospheric ozone (O_3) is one of the most problematic air pollutants over Europe with up to 98 % of Europe's urban population exposed to concentrations of ozone above the WHO guidelines (EEA, 2015). Furthermore, in 2011 the EU ozone target value for human health (the EU has no limit value for ozone) was exceeded in 65 % of the EU member states and Europe's ozone target value for vegetation was exceeded in 27 % of the EU-28 agricultural areas (EEA, 2013).

Reducing atmospheric concentrations of tropospheric ozone is a complex problem as ozone is not directly emitted into the troposphere. Tropospheric ozone is produced from the reactions of volatile organic compounds (VOCs) in the presence of nitrogen oxides ($NO_x \equiv NO + NO_2$) and sunlight (Atkinson, 2000). Meteorology and transport also influence tropospheric ozone levels (Jacob and Winner, 2009).

Air quality (AQ) models are an important tool for understanding ozone pollution and predicting future air quality. Many AQ models are available with different scales and dimensions depending on the scope of the modelling experiment. Accurately representing the complexity of ozone production in a computationally efficient model is an ongoing challenge for the modelling community (Russell and Dennis, 2000).

Model intercomparison projects (MIPs) compare the outputs from different models showing differences in tropospheric ozone due to differing representations of key processes. For example, ACCMIP (Atmospheric Chemistry and Climate Model Intercomparison Project) showed different magnitudes of future ozone burden in the same region (Young et al., 2013). A current MIP, CCMI (Chemistry Climate Model Initiative), aims to investigate differences in the representation of chemistry, emissions and transport processes between models to understand the differences between predictions from global models (Eyring et al., 2013).

Detailed process studies are key to understanding differences between simulated ozone levels using different models. This thesis determines the effects of VOC degradation chemistry, VOC emissions and temperature on modelled ozone predictions. This assessment should be beneficial to the modelling community in understanding potential differences between model outputs and improving AQ models.

1.1 Ozone

Ozone is a atmospheric gas found in the stratosphere and troposphere, however its atmospheric effects are very different in these regions. The stratosphere contains $\sim$ 90 % of the atmospheric ozone with a peak mixing ratio of $\sim$ 12 ppm (Seinfeld and Pandis, 2006). Stratospheric ozone absorbs the sun's ultraviolet radiation which is important due to the adverse effects of excess UV radiation on humans and ecosystems.

In contrast, tropospheric (or surface) ozone is both a pollutant and a greenhouse gas. Increased levels of tropospheric ozone are harmful to humans, plants and other living systems. High ozone exposure may lead to pulmonary problems in humans and can decrease both crop yields and forest growth (World Meteorological Organisation, 2011).

Tropospheric ozone is formed via photochemical production from the reactions between VOCs and NO_x, described in Sect. 1.2, while meteorology and atmospheric transport also influence ozone concentrations. For example, a spring-time peak in tropospheric ozone is common in the Northern Hemisphere (NH) mid-latitudes, originally attributed to transport of ozone from the stratosphere into the troposphere via the Stratosphere-Troposphere Exchange (STE) (Monks, 2000). However, ozone transported via STE rarely influences surface ozone levels (Lelieveld

and Dentener, 2000) and the spring maximum is due to the photochemical reactions occuring in the NH spring after the buildup of reservoir species over winter (Penkett and Brice, 1986).

Understanding the intracacies of surface ozone pollution requires a combined effort from the modelling, observational and chemical kinetic communities – called the "three-legged stool" approach by Abbatt et al. (2014). Modelling of ozone production helped understand the complexity of atmospheric chemistry, such as the non-linear relationship of ozone production with precursor (VOC and NO_x) emissions. Modelling studies attempt to reproduce observational trends of surface ozone and model predictions may inform new observational studies. Chemical kinetic studies performed by laboratories give insights to missing or incorrect representations of atmospheric chemistry to be included in updated models.

This thesis focuses on the influence on ozone production from the representation of VOC degradation chemistry, VOC emissions and the ozone-temperature relationship within models. Ozone production chemistry is outlined in Sect. 1.2, while sources of emissions of ozone precursors are described in Sect. 1.3. Finally, the effects of meteorology on ozone production are presented in Sect. 1.4. For the rest of this thesis, ozone refers to tropospheric ozone.

1.2 Ozone Chemistry

Ozone absorbs UV radiation producing either ground-state atomic oxygen ($O(^3P)$) or excited singlet ($O(^1D)$) oxygen atoms.

$$O_3 + h\nu \rightarrow O_2 + O(^3P) \quad \text{(R1)}$$

$$O_3 + h\nu \rightarrow O_2 + O(^1D) \quad \text{(R2)}$$

Ground-state oxygen quickly reacts with oxygen to reform ozone.

$$O(^3P) + O_2 \xrightarrow{M} O_3 \quad \text{(R3)}$$

Thus there is no net loss or production of ozone through (R1) and (R3). $O(^1D)$ may collide with N_2 or O_2 (represented as M in chemical reactions) stabilising to the ground-state. This process again leads to a null cycle with ozone destruction balanced by production. However, $O(^1D)$ can react with water vapour producing hydroxyl (OH) radicals. The OH radical is a highly reactive chemical species reacting with almost all trace chemical species in the troposphere. (Seinfeld and Pandis, 2006;

Monks, 2005)

$$O(^1D) + H_2O \rightarrow 2\,OH \tag{R4}$$

The initial oxidation of VOCs by OH initiates a reaction chain which may lead to net production or loss of ozone depending on the atmospheric conditions. For example, when carbon monoxide (CO) reacts with OH in the presence of oxygen, carbon dioxide and the hydroperoxy (HO_2) radical are formed. In polluted areas with high-NO_x concentrations, HO_2 readily reacts with nitrogen oxide (NO) regenerating OH and producing nitrogen dioxide (NO_2).

$$CO + OH \xrightarrow{O_2} HO_2 + CO_2 \tag{R5}$$

$$HO_2 + NO \rightarrow OH + NO_2 \tag{R6}$$

Photolysis of NO_2 produces ground-state atomic oxygen leading to ozone production via (R3).

$$NO_2 + h\nu \rightarrow NO + O(^3P) \tag{R7}$$

The reaction between OH and NO_2 produces nitric acid (HNO_3) limiting the recycling of OH and NO_2. Nitric acid may be removed through deposition processes and is a sink for both OH and NO_2.

$$NO_2 + OH \rightarrow HNO_3 \tag{R8}$$

In low-NO_x conditions away from polluted areas, OH and HO_2 are interconverted through reactions with ozone.

$$OH + O_3 \rightarrow HO_2 + O_2 \tag{R9}$$

$$HO_2 + O_3 \rightarrow OH + 2\,O_2 \tag{R10}$$

OH and HO_2 may also react in a termination reaction producing water vapour and oxygen.

$$HO_2 + OH \rightarrow H_2O + O_2 \tag{R11}$$

Other termination reactions involve combination reactions of HO_2 radicals producing hydrogen peroxide (H_2O_2).

$$HO_2 + HO_2 \rightarrow H_2O_2 \tag{R12}$$

Hydrogen peroxide may be removed through deposition (Gunz and Hoffmann, 1990)

Figure 1.1: Methane degradation pathways in low-NO_x and high-NO_x conditions. Taken from Monks (2005).

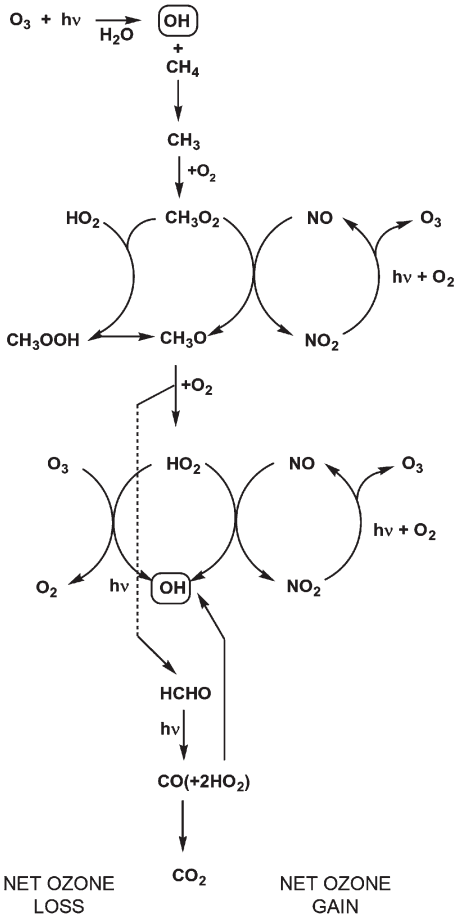

but may also be a temporary sink for the odd-oxygen species OH and HO_2.

$$H_2O_2 + h\nu \rightarrow 2\,OH \tag{R13}$$

$$H_2O_2 + OH \rightarrow HO_2 + H_2O \tag{R14}$$

In summary, the secondary degradation of CO produces ozone in high-NO_x conditions while in low-NO_x conditions ozone is destroyed. (Seinfeld and Pandis, 2006; Monks, 2005)

The secondary degradation of more complex VOCs has similar features to that of CO. Methane (CH_4), with a mixing ratio of $\sim$ 1.7 ppmv, is the most abundant VOC in the troposphere. The reaction of CH_4 with OH, in the presence of O_2, produces the methyl peroxy radical (CH_3O_2) – the simplest organic peroxy radical (RO_2).

$$CH_4 + OH \xrightarrow{O_2} CH_3O_2 + H_2O \tag{R15}$$

Similar to CO oxidation, NO_x conditions play a crucial role in the fate of CH_3O_2

Figure 1.2: Schematic diagram outlining general pathways of the secondary degradation of an emitted VOC.

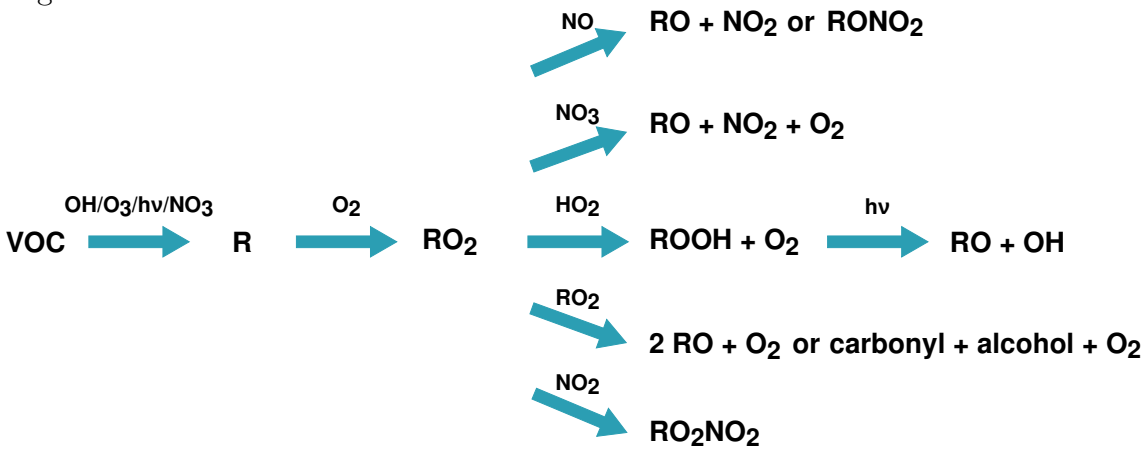

and whether ozone is produced or destroyed, depicted in Fig. 1.1.

The general types of secondary degradation products formed during CH_4 degradation can be extended to more complex non-methane VOCs (NMVOCs). Initial oxidation pathways of NMVOCs are reaction with OH, while unsaturated VOCs, such as alkenes, may react with ozone and photolysis is important for carbonyl species. During the night-time, reaction with the nitrate (NO_3) radical is typically more important than OH-oxidation due to the relatively higher night-time concentrations of NO_3.

$$\mathrm{VOC} + \mathrm{OH/NO_3/O_3/h\nu} \xrightarrow{\mathrm{O_2}} \mathrm{RO_2} \tag{R16}$$

Figure 1.2 represents a general and simplified reaction scheme for VOCs in the troposphere. The initial oxidation of NMVOC produces RO_2 radicals and the fate of the RO_2 determines whether net loss or production of ozone occurs.

$$\mathrm{RO_2 + NO} \xrightarrow{\mathrm{M}} \mathrm{RONO_2} \tag{R17}$$

$$\mathrm{RO_2 + NO} \rightarrow \mathrm{RO + NO_2} \tag{R18}$$

$$\mathrm{RO_2 + NO_2} \underset{}{\overset{\mathrm{M}}{\rightleftharpoons}} \mathrm{RO_2NO_2} \tag{R19}$$

$$\mathrm{RO_2 + NO_3} \rightarrow \mathrm{RO + NO_2 + O_2} \tag{R20}$$

$$\mathrm{RO_2 + HO_2} \rightarrow \mathrm{ROOH + O_2} \tag{R21}$$

$$\mathrm{RO_2 + RO_2} \rightarrow \mathrm{2\,RO + O_2} \tag{R22}$$

$$\mathrm{RO_2 + RO_2} \rightarrow \mathrm{RCH(OH)R + RC(O)R + O_2} \tag{R23}$$

All degradation pathways of RO_2 that produce NO_2 result in O_3 formation due to (R7) and (R3). Reaction with HO_2 forms a hydroperoxide (ROOH) which may either

be deposited or photolysed producing an alkoxy (RO) radical and OH. The carbonyl and alcohol products resulting from reactions between RO_2 radicals follows a similar sequence of reactions and can produce further O_3. Thus the subsequent reactions of secondary degradation products of a VOC may lead to further production of ozone.

Reaction of RO_2 with NO_2 (R19) forms peroxy nitrates (RO_2NO_2) which are a temporary reservoir for RO_2 and NO_x. The thermal decomposition rate of RO_2NO_2 is highly temperature dependent. At lower temperatures, RO_2NO_2 builds up and may be transported away from the region of formation. Thus releasing RO_2 and NO_2 in areas away from large sources of NO_x and fuelling ozone production.

The reaction between NO and ozone is another important reaction in polluted regions.

$$NO + O_3 \rightarrow NO_2 + O_2 \qquad \text{(R24)}$$

Together with (R7) and (R3), (R24) form a null cycle of ozone production and destruction which limits ozone levels. On the local urban scale close to NO sources, (R24) decreases ozone levels called ozone titration. Ozone titration is also important during the night where the lack of photochemistry does not regenerate ozone. Urban measurement studies have confirmed the importance of ozone titration near sources of NO (Syri et al., 2001).

1.2.1 VOC and NO_x Chemistry

The chemistry in low-NO_x and high-NO_x conditions indicates that ozone production is a non-linear process. Figure 1.3, from Jenkin and Clemitshaw (2000), depicts the non-linear relationship between ozone as a function of VOC and NO_x. This relationship can be divided into distinct regimes of ozone production: *NO_x-sensitive* (or *NO_x-limited*), *NO_x-saturated* (or *VOC-limited*) and *VOC-and-NO_x-sensitive* regimes.

In regions with low-NO_x concentrations, RO_2 are more likely to react with other radicals rather than convert NO to NO_2 leading to ozone production. Increasing NO_x levels increases the number of NO to NO_2 conversions by peroxy radicals leading to ozone production. While, increasing VOC levels has little effect on O_3 production due to increased radical-radical reactions. This is *NO_x-sensitive* chemistry.

On the other hand in regions with high levels of NO_x, reactions between radicals and NO_x are more likely to occur. The production of HNO_3 increases through

Figure 1.3: Ozone isopleth plots for various initial mixing ratios of NO_x and VOCs. Taken from Jenkin and Clemitshaw (2000).

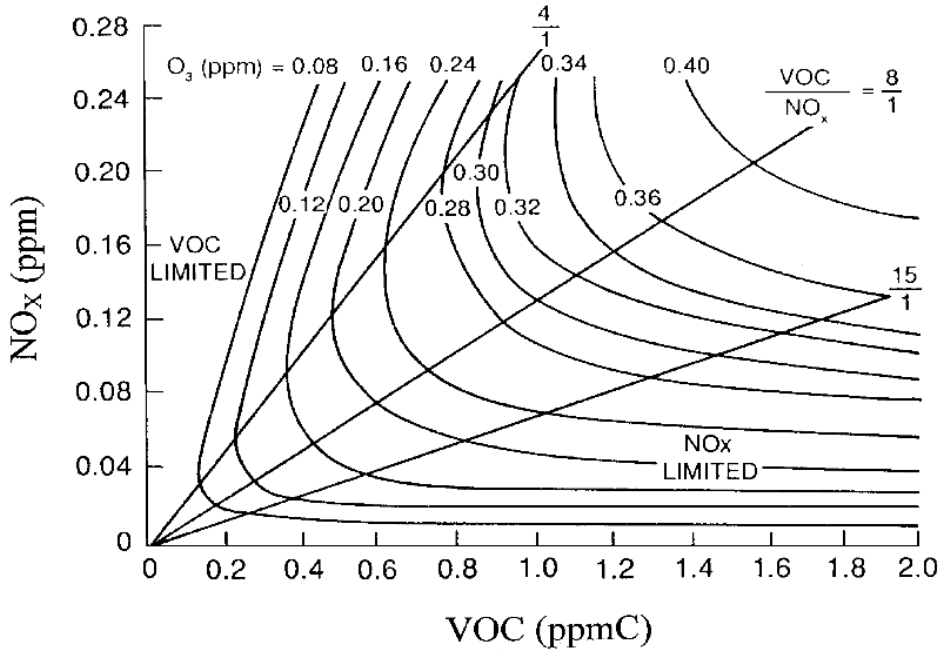

(R8) removing OH and NO_x. Increasing levels of VOC increase the likelihood of RO_2 converting NO to NO_2 leading to ozone production while increasing NO_x levels will not increase O_3 production. This is *NO_x-saturated* or *VOC-limited* chemistry.

The VOC-and-NO_x-sensitive regime (contour ridges in Fig. 1.3) is characterised by O_3 production being sensitive to both VOC and NO_x levels. Morever, it is in this atmospheric regime that the maximum amount of ozone is produced. Kleinman (1994) showed that this non-linear relationship can be thought of as a titration process between radicals and NO_x with the VOC-and-NO_x-sensitive regime being the turning point.

The non-linear nature of ozone production is one of the challenges in controlling ozone levels. The difficulty is exacerbated by the fact that the troposphere can alternate between these regimes depending on the meteorological conditions. Moreover, fresh emissions tend to occur in NO_x-saturated areas before being transported to VOC-and-NO_x-sensitive and NO_x-sensitive regions.

1.2.2 Representing Atmospheric Chemistry in Models

Representing the degradation chemistry for each VOC in a chemical transport model (CTM) is unrealistic. Even if all the secondary degradation pathways

and products were known for every VOC, a CTM is unable to efficiently solve the differential equations.

The representation of atmospheric chemistry in a CTM is called a chemical mechanism. Chemical mechanisms are developed by simplifying and aggregating VOCs, degradation products and reactions. Less aggressive simplification approaches may result in a chemical mechanism having thousands of species while more aggressive simplification may result in only a hundred species. Chemical mechanisms are verified by comparing the concentrations of field studies or controlled chamber study experiments to model simulations (Stockwell et al., 2012). Section 2.2 includes further details of the simplification techniques used to develop chemical mechanisms.

Chemical mechanism comparison studies, such as Kuhn et al. (1998) and Emmerson and Evans (2009), compared the outputs of different chemical mechanisms using the same model setup and initial conditions. These studies showed that the differences between chemical mechanisms led to large differences in simulated ozone concentrations. While these comparisons indicate that chemical mechanisms lead to differences in ozone levels, they do not point out the root cause of the differences.

Determining the source of differences between chemical mechanisms is a difficult task due to the interlinked chemistry of many key species. As part of this study, the ozone production from different chemical mechanisms is compared and differences in the treatment of VOC degradation chemistry is determined. The research questions driving this comparison are presented in Sect. 1.5 and the results are described in Sect. 3.1.

1.3 Source and Sinks of Ozone Precursors

Ozone precursors are emitted from many anthropogenic and biogenic sources with varying emissions throughout the year, month or time of day. In many regions, reduced road transport during the weekend leads to a noticible reduction in NO_x emissions influencing ozone levels. This is called the "weekend-effect". For example, ozone production is NO_x-saturated during weekdays in San Joaquin Valley, California but during the weekend higher ozone levels are recorded as the reduction in NO_x levels leads to VOC-and-NO_x-sensitive chemistry (Pusede et al., 2014). Many sources of NMVOC, such as industry and solvent use, also reduce activities during the weekend. Residential combustion is highest during the winter months and lowest during the summer (Denier van der Gon et al., 2011).

Figure 1.4: The sources and sinks of NO_x, adapted from Seinfeld and Pandis (2006).

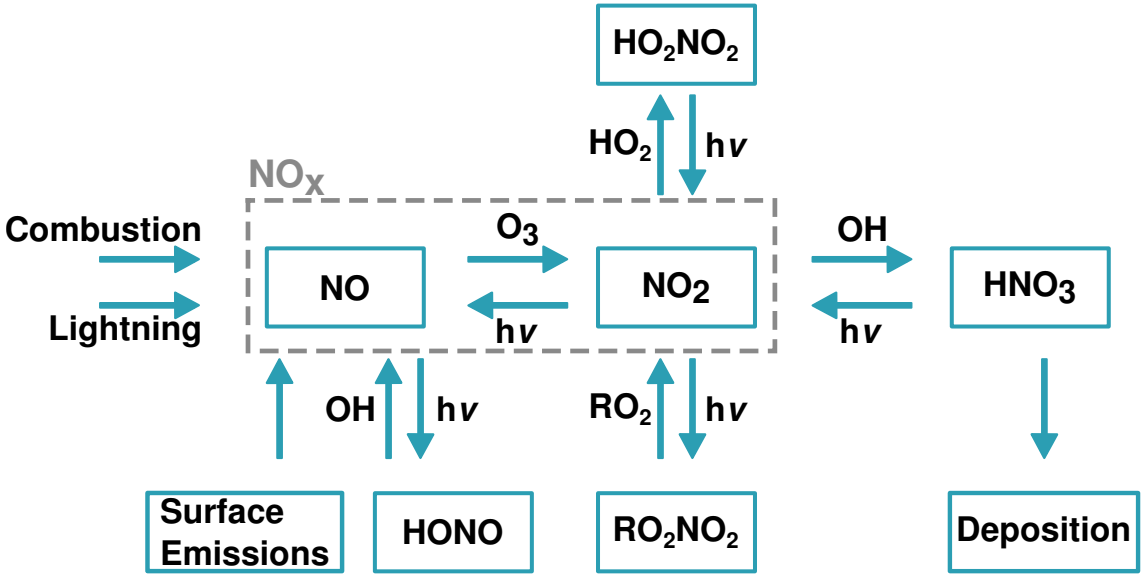

1.3.1 NO_x

Anthropogenic activities are the main source of NO_x emissions into the atmosphere. In the year 2000, almost 52 Tg N were emitted with 65 % through fossil fuel combustion (Seinfeld and Pandis, 2006). Examples of fossil fuel combustion emitting NO_x are transportation using diesel or petrol vehicles, industrial activities and domestic heating (von Schneidemesser et al., 2015).

Up to 95 % of NO_x emissions from combustion are emitted as NO, which is oxidised to form NO_2 through (R24) and (R6). However, the increase in diesel vehicles and the implementation of diesel filters increased the fraction of emitted NO_2 from vehicles. Grice et al. (2009) showed that over Europe, emissions of NO_2 from diesel vehicles have increased from 8.6 % in 2000 to 12.4 % in 2004.

Despite the majority of NO_x emissions coming from human activities, there are also natural sources of NO_x. Lightning is an important source of NO_x in the free troposphere while emissions of NO_x from soils are important in remote regions with little anthropogenic influence. Lightning and soils each contributed $\sim$ 10 % to global NO_x emissions in 2000 (Seinfeld and Pandis, 2006).

The main sink of NO_x is deposition of nitric acid, formed via (R8). Temporary reservoirs, such as peroxy nitrates and HONO, may be transported away from sources into areas devoid of large sources of NO_x. These sources and sinks of NO_x are illustrated in Fig. 1.4.

1.3.2 VOCs

The main sink of VOCs is the oxidation chemistry described in Sect. 1.2. The degradation of a VOC yields the maximum possible amount of ozone when every peroxy radical converts NO to NO_2 called the *ozone production potential* (OPP) of a VOC. In reality, the OPP of a VOC is never achieved as other reactions with peroxy radicals occur however the OPP is useful for assessing the amount of ozone produced from emitted VOCs.

Carbon Monoxide

Carbon monoxide is emitted directly into the troposphere through combustion and industrial processes. An equally-important source of CO is its formation during VOC degradation. Hauglustaine et al. (1998) estimated that 881 Tg yr^{-1} of CO was produced globally from chemical oxidation of VOC while 1219 Tg yr^{-1} of CO was directly emitted.

The reaction between CO and OH (R5) is the main sink of CO. The OPP of CO is one as the degradation of CO produces one peroxy radical (HO_2), thus a maximum of one molecule of ozone may be produced during CO degradation.

Methane

Emissions of methane range between 500 and 600 Tg CH_4 yr^{-1} with ~ 60 % of the emissions from anthropogenic sources. The main anthropogenic sources of CH_4 are agriculture, fossil fuels and biomass burning with agriculture contributing 60 % of the anthropogenically emitted CH_4. Emissions from wetlands are the main natural source of methane emissions (Kirschke et al., 2013).

Methane has a lifetime of about 9 years, significantly longer than other VOCs. Thus, methane influences ozone production on the global rather than the regional scale.

Reaction with OH (R15) is the main sink of methane and the secondary degradation of CH_4 (Fig. 1.1) produces CO and four peroxy radicals ($1\times$ CH_3O_2, $3\times$ HO_2). Thus the OPP of methane is five as methane degradation can produce a maximum five molecules of O_3 per molecule of CH_4 oxidised.

NMVOCs

A wide variety of NMVOCs are emitted from anthropogenic activities directly into the troposphere. Solvent use, industry, fossil fuel burning and transportation are all major activities emitting NMVOCs of varying functional groups, carbon numbers and reactivity. Emissions of NMVOC from vegetation depends on meteorological variables (such as, temperature and radiation) and biological variables (such as, leaf age and leaf area index) (Guenther et al., 2012).

Lamarque et al. (2010) estimated that in 2000, 130 Tg NMVOC were globally emitted from anthropogenic sources. This amount is dwarfed by emissions from biogenic sources – 1000 Tg NMVOC yr^{-1} (Guenther et al., 2012). Isoprene (C_5H_8) emitted from vegetation dominates at the global scale however emissions of monoterpenes and sesquiterpenes from vegetation may also be significant.

Although isoprene is considered as a biogenic VOC (BVOC), it has been measured in the urban areas of London and Paris away from biogenic emission sources. Transport of isoprene is unlikely as isoprene is a highly reactive NMVOC indicating anthropogenic sources of isoprene (von Schneidemesser et al., 2011). Other NMVOC emitted from anthropogenic sources, such as methanol and acetaldehyde, are also emitted from vegetation (Guenther et al., 2012).

The maximum number of molecules of O_3 produced per degradation of an emitted NMVOC depends on the type and the number of carbons of the NMVOC leading to a wide range of OPPs for different NMVOC. Unsaturated NMVOC, such as alkenes, tend to have larger OPPs than alkanes (saturated NMVOC). Even within a functional group of NMVOC different OPPs are calculated. For example, benzene and xylene are both aromatic compounds but as benzene is a more chemically stable molecule it has a lower OPP than xylene (Carter, 1994).

OPPs for complex NMVOCs are calculated using models by incrementally varying the concentration of an NMVOC and calculating the change in ozone. Different OPP scales have been developed using different NO_x conditions. The Maximum Incremental Reactivity (MIR) and Maximum Ozone Incremental Reactivity scales of Carter (1994) and the Tagged Ozone Production Potential (TOPP) are examples of OPP scales for NMVOCs.

Table 1.1: Emission source sectors for anthropogenic emissions listed in the TNO_MACCIII inventory (Kuenen et al., 2014).

Description	**Description**
Public Power	Road Transport: Others
Residential Combustion	Road Transport: Evaporation
Industry	Road Transport: Wear
Fossil Fuel	Non-road Transport
Solvent Use	Waste
Road Transport: Gasoline	Agriculture
Road Transport: Diesel	

1.3.3 Representing NMVOC Emissions in Models

Emissions of NMVOC species are a critical input in models and emission inventories are used to specify the type and quantity of emissions from source categories. Table 1.1 lists the source sectors of emissions used by the TNO_MACCIII emission inventory (Kuenen et al., 2014). Emission inventories are available for the global or regional emissions. For example, EDGAR (Olivier et al., 2001) specifies global emissions while TNO_MACCIII (Kuenen et al., 2014) specifies European emissions.

Many uncertainties are associated with emission inventories. For example, Coll et al. (2010) showed that large discrepancies arise between ambient measurements and emission inventories. Also, the temporal variation of emissions are not captured by emission inventories (Boynard et al., 2014).

BVOC emissions depend on meteorolgical and biological variables and algorithms estimating BVOC emissions may be calculated as part of the model simulation instead of an emission inventory. The Model of Emissions of Gases and Aerosols from Nature (MEGAN) (Guenther et al., 2006, 2012) calculates BVOC emissions using the temperature and radiation values determined from the model. Specifiying BVOC emissions using an algorithm or emission inventory influences modelled ozone concentrations. For example, Curci et al. (2009) noted large differences in summertime ozone concentrations over Europe when using a gridded emission inventory or an on-line algorithm for BVOC emissions.

Emissions of the NMVOCs specified by an emission inventory are mapped to the chemical mechanism species used in the model. This mapping is not standardised throughout the modelling community with the same NMVOC emissions possibly being allocated to different chemical species even if using the same chemical mechanism (Carter, 2015).

Table 1.2: Influence of meteorological variables on ozone production, taken from Jacob and Winner (2009).

Meteorological Variable	Influence on Ozone
Temperature	Consistently positive
Stagnation	Consistently positive
Wind Speed	Generally negative
Mixing Height	Weak or variable
Humidity	Weak or variable
Cloud Cover	Generally negative
Precipitation	Weak or variable

The influence of the speciation of NMVOC emissions on modelled ozone production is determined as part of this work. Moreover, the effect of using the same speciations of NMVOC emissions with different chemical mechanisms is also explored. Section 1.5 outlines the research questions and the results are presented in Sect. 3.2.

1.4 Effects of Meteorology on Ozone Production

Meteorological conditions influence the production of ozone with clear and calm summer days typically having high ozone levels (Dueñas et al., 2002). Comrie (1997) noted a complex relationship between meteorology and ozone due to competing positive and negative effects on ozone production. Table 1.2, taken from Jacob and Winner (2009), details the effects of specific meteorological variables on ozone production.

Climate change is predicted to influence many meteorological variables and increase the number of heatwaves. Thus understanding the influence of meteorology on ozone production is particularly important for future predictions of air quality and tackling ozone pollution in a changing climate.

Humidity

Humidity influences ozone production both positively and negatively. When $O(^1D)$, originating from ozone photolysis (R2) reacts with water vapour (R4), the production of OH radicals leads to ozone loss. However, the initiation of VOC degradation through reaction with OH can lead to ozone production (Sect. 1.2). These competing effects of water vapour on ozone production lead to a weak correlation of ozone production with water vapour (Jacob and Winner, 2009).

Wind Speed

High wind speeds transport ozone precursors away from their sources leading to a generally negative effect on ozone pollution over a region. Model projections of Doherty et al. (2013) showed that while climate change is expected to change large-scale atmospheric transport there is little influence on the spatial patterns of mean concentrations of ozone.

Stagnation

During periods of low wind speeds, emissions of ozone precursors remain close to their sources. These stagnant conditions over polluted urban areas are highly correlated with increased ozone production over urban areas (Jacob and Winner, 2009). Heatwaves result from stagnant conditions along with high temperatures enhancing the ozone pollution over a region.

Mixing Height

The effects of the mixing height of the planetary boundary layer (PBL) with the free troposphere depend on the region. For example, Dawson et al. (2007) found that over the Eastern U.S., regions with low ozone are positively correlated with mixing height whereas regions with high ozone levels are negatively affected. This spatial effect of mixing height on ozone production depends on the difference between ozone levels within the PBL and the free troposphere (Jacob and Winner, 2009).

Mixing between the PBL and free troposphere into regions with levels of surface ozone lower than the free troposphere is an additional source of ozone. Conversely, mixing of the elevated levels of ozone from polluted areas into the free troposphere reduces the burden of surface ozone.

Temperature

Temperature is positively correlated with ozone in many areas. Otero et al. (2016) showed that temperature was the main driver of summertime ozone values over many areas of central Europe while Camalier et al. (2007) correlated ozone with temperature over the Eastern US. Sillman and Samson (1995) illustrated that only

ozone pollution produced from the chemistry described in Sect. 1.2 is correlated with temperature rather than background ozone, the ozone levels without the influence of anthropogenic emissions.

Temperature directly influences ozone levels in two ways: increasing the emissions of VOCs from vegetation and speeding up the rates of chemical reactions. The review of Pusede et al. (2015) showed that the temperature dependence of radical production, organic reactivity, the shorter lifetime of RO_2NO_2 and the formation of alkyl nitrates (R18) affects ozone production.

There is a lack of detailed process studies separating the direct effects of temperature on ozone over differing NO_x conditions despite observational and regional modelling studies correlating temperature with ozone production. The final part of this work addresses whether the increase in BVOC emissions or faster reaction rates with temperature is more important for ozone production. The research questions for this study are detailed in Sect. 1.5 and results are presented in Sect. 3.3.

1.5 Research Questions

The detailed chemistry producing ozone cannot be fully represented in models for reasons of computational efficiency. Thus models select a particular representation of atmospheric chemistry raising the overarching research questions for this thesis:

- How do representations of detailed atmospheric chemistry influence simulated ozone production?
- What are the most important chemical processes when simulating ozone production?

This question is addressed in this work through detailed modelling studies highlighting the chemical processes having the largest impact on simulated ozone production under three different conditions.

Firstly, different simplified versions of the ozone production chemistry are available to the modelling community with comparison studies showing that ozone concentrations vary between chemical mechanisms. These chemical mechanism comparison studies do not determine the root causes of the differences between chemical mechanism, leading to the research questions:

- How do the simplification techniques used by different chemical mechanisms

affect ozone production?
- Which processes are responsible for differences in ozone production with different chemical mechanisms?

Secondly, NMVOC emissions are a known source of uncertainty in modelling experiments. The choice of emission inventory influences the speciation of individual NMVOC emissions possibly influencing ozone production. By comparing the ozone produced using different emission inventories, the following research questions are addressed:

- What is the influence on modelled ozone production when using different speciations of emitted NMVOCs?
- Does this influence change when using different chemical mechanisms?

Finally, meteorology influences ozone production with temperature having the strongest positive correlation with ozone. Temperature directly influences ozone production through increasing biogenic emissions and speeding up the reaction rates of chemical reactions.

- Are temperature-dependent emissions or chemical processes more important for ozone production with increasing temperature?
- How is the ozone-temperature relationship treated by different chemical mechanisms?

Detailed processed studies were performed using a box model to address these research questions, details of the experimental setup are presented in Chap. 2. The results of the experiments are found in Chap. 3, the general discussion and conclusions of the thesis are in Chap. 4.

Chapter 2

Methodology

This chapter details the methodology used to address the research questions of this work (Sect. 1.5). A brief description of AQ modelling followed by the model set-up used in the separate studies (Sect. **??**). The chemical mechanisms used in this work are introduced in Sect. **??** and the required initial and boundary conditions are described in Sect. 2.3

2.1 Air Quality Modelling

AQ models are mathematical representations of the atmosphere designed to produce continuous output fields that aid in explaining sources of air pollution. All models numerically solve the system of differential equations describing the conservation of chemical species used by the model (Russell and Dennis, 2000).

Solving the system of differential equations requires initial and boundary conditions for each chemical species. Initial conditions fix the starting concentrations of each species in every grid-box. Boundary conditions require knowledge of the concentration and transport of each species at the boundary edges of the model grid.

Eulerian models are the most common type of AQ model (Russell and Dennis, 2000). These models describe the atmosphere by fixed grid-boxes where species are transported in and out of the boxes (Seinfeld and Pandis, 2006). Box models are the simplest type of model (zero-dimensional) having uniform atmospheric concentrations that are a function of time. Whereas 3-D models describe atmospheric concentrations as a function of time, latitude, longitude and height requiring more computing power than a box model (Seinfeld and Pandis, 2006). Box models may

Table 2.1: MECCA box model settings.

Model Parameter	Setting
Pressure	1013 hPa
Relative Humidity	81 %
Starting Date and Time	27th March 06:00
Model Time Step	20 mins

lack realism but are useful for studying detailed processes influencing air quality.

2.1.1 Model Description and Setup

The MECCA (Module Efficiently Calculating the Chemistry of the Atmosphere) box model was used throughout this work. MECCA was developed by Sander et al. (2005) and adapted to include MCM v3.1 chemistry by Butler et al. (2011). MECCA was used in the published studies of Kubistin et al. (2010) and Lourens et al. (2016).

MECCA is written in Fortran code and runs on UNIX/Linux platforms. The Kinetic Pre-Processor (KPP, Damian et al. (2002)) processed the chemical mechanism and generated Fortran code further compiled within MECCA. KPP has many choices of numerical solver for solving the differential equations, a Rosenbrock solver (ros3 option) was used throughout this work.

Emissions of species into the box and deposition of species out of the box were handled by KPP. The chemical mechanism included pseudo-unimolecular reactions specifying the emissions and dry deposition of chemical species with the relevant rate. The emitted chemical species and emission rates were read into the model using a namelist file. Namelist files also specified the initial and boundary conditions of chemical species.

The physical parameters used in MECCA throughout this work are detailed in Table 2.1. In the first two studies, temperature was held constant at 293 K and the boundary layer height was fixed at 1000 m. In the final study, MECCA was updated to include a diurnal boundary layer height and temperature was systematically varied between 288 and 313 K (15–40 °C). These changes to the model setup for the final study are outlined in Paper III (Chap. 8).

Photolysis rates were paramaterised as a function of the solar zenith angle based on the approach of the MCM (Jenkin et al., 1997). This paramaterisation

Table 2.2: Chemical mechanisms used in this work.

Chemical Mechanism	Lumping Type	Reference
MCM v3.1 and v3.2	No lumping	Jenkin et al. (1997), Jenkin et al. (2003) Saunders et al. (2003), Bloss et al. (2005) Rickard et al. (2015)
CRIv2	Lumped intermediate	Jenkin et al. (2008)
MOZART-4	Lumped molecule	Emmons et al. (2010)
RADM2	Lumped molecule	Stockwell et al. (1990)
RACM	Lumped molecule	Stockwell et al. (1997)
RACM2	Lumped molecule	Goliff et al. (2013)
CBM-IV	Lumped structure	Gery et al. (1989)
CB05	Lumped structure	Yarwood et al. (2005)

utilises the degree of latitude and in the first two studies 34 °N, roughly the city of Los Angeles, was used. In the final study, the latitude was set to 51 °N simulating central European conditions.

2.2 Chemical Mechanisms

The chemical mechanisms used in this study are listed in Table 2.2 with more details found in Paper I (Sect. 3.1). These chemical mechanisms were chosen as they are commonly used by the AQ modelling community as outlined by the review of European modelling groups by Baklanov et al. (2014).

The Master Chemical Mechanism (MCM, Jenkin et al. (1997, 2003); Saunders et al. (2003); Bloss et al. (2005); Rickard et al. (2015)) is a near-explicit chemical mechanism with a high level of detail making it ideal as the reference chemical mechanism in each study of this work. The Common Representative Intermediates (CRI) chemical mechanism (Jenkin et al., 2008) is an lumped intermediate mechanism where the degradation productions are aggregated (lumped) rather than emitted VOC.

Lumped molecule chemical mechanisms aggregate primary VOC into mechanism species and is the most commonly used simplification technique. The lumped-molecule chemical mechanisms used in this work were Model for OZone and Related chemical Tracers (MOZART, Emmons et al. (2010)), Regional Acid Deposition Model (RADM2, Stockwell et al. (1990)), Regional Atmospheric Chemistry Mechanism (RACM, Stockwell et al. (1997)) and RACM2 Goliff et al. (2013). Lumped structure chemical mechanism represent emissions of NMVOC through emissions of mechanism species representing the bonds present in the NMVOC. The Carbon Bond mechanisms CBM-IV (Gery et al., 1989) and CB05 (Yarwood et al., 2005)

were the lumped-structure chemical mechanisms used in this work.

2.2.1 Implementing Chemical Mechanisms in MECCA

Each chemical mechanism listed in Table 2.2 was adapted to the KPP format used in the MECCA box model. The WRF-Chem model (Grell et al., 2005) includes KPP versions of RADM2, RACM and CBM-IV and this was the source for these chemical mechanisms. The full version of the CRI v2 was obtained from `http://mcm.leeds.ac.uk/CRI` while the original reference was the source for all other chemical mechanisms in Table 2.2.

In order to focus on the differences in the representation of VOC degradation between the chemical mechanisms, a number of harmonisations between the chemical mechanisms were implemented. For these harmonisations, the approaches used by the reference chemical mechanism (MCM v3.2) were implemented in the reduced chemical mechanisms. These changes are detailed in Paper I (Chap. 6).

2.2.2 Tagging of Chemical Mechanisms

AQ models can be used to allocate the effects of different precursors or emission sources on ozone production. For example, source removal studies perform separate model simulations with and without emissions from a sector to quantify the effect of the sector on ozone production, such as the quantification of megacity emissions on ozone production in Butler and Lawrence (2009). Tagging is another approach where the chemical mechanism includes additional chemical species labelled (tagged) with source information. For example, Emmons et al. (2012) tagged the MOZART-4 chemistry to attribute ozone production to emission sources of NO_x.

In Butler et al. (2011), tagged VOC chemistry allows allocation of ozone production to emitted VOC. Tagging involves labelling every organic degradation product produced during the degradation of a VOC with the name of the VOC. This labelling is repeated for every degradation product until the final degradation products (CO_2 and H_2O) are produced, thus every VOC has a separate set of reactions fully describing its degradation. This tagging approach uses O_x production as a proxy for O_3 production and is only valid for NO_x-limited and VOC-and-NO_x sensitive chemistry not NO_x-saturated conditions. The O_x family includes O_3, NO_2, $O(^1D)$, $O(^3P)$, NO_3, N_2O_5 and other species involved in fast production and loss cycles with NO_2.

All chemical mechanisms in Table 2.2 were tagged using the approach of Butler et al. (2011). In the first study, the tagging approach was the basis for comparing the respresentations of VOC degradation chemistry and their effects on ozone production. The second study used VOC-and-NOx-sensitive conditions and simulations using the tagged chemical mechanisms determined sources of differences in ozone production from the solvent sector emission inventories of Table 2.3. Variable NO_x conditions were used in the third study hence using the tagging approach was not possible. Thus all model simulations assessing the ozone-temperature relationship with different NO_x conditions were performed with non-tagged versions of the chemical mechanisms.

2.3 Initial and Boundary Conditions

In all simulations of this work, methane (CH_4) was fixed to 1.75 ppmv while carbon monoxide (CO) and O_3 were initialised at 200 ppbv and 40 ppbv and then allowed to evolve freely. The initial conditions for NMVOC emissions were held constant until noon of the first day of simulations to simulate a fresh emissions plume.

NMVOC Initial Conditions

The initial conditions for NMVOC species differed in each experiment, a brief summary is given below and details are found in the respective publications (Chaps. 6–8). The first study used the initial conditions of the Los Angeles simulation in Butler et al. (2011) to determine the emissions needed for constant mixing ratios of the initial NMVOCs. These emissions were mapped to the appropriate chemical species of each chemical mechanism in Table 2.2 keeping the amount of emitted NMVOC constant between model runs.

The second study used NMVOC emissions specified by the emission inventories for the solvent sector listed in Table 2.3 over a theoretical urban area of 1000 km^2 with total NMVOC emissions of 1000 tons/day. The solvent sector contributes $\sim$ 43 % by mass of total emissions (EEA, 2011), thus total NMVOC emissions of 430 tons/day were used. Further simulations used emissions from all other sectors (remaining 570 tons/day) while varying the solvent sector NMVOC emissions. Additional simulations included BVOC emissions of isoprene and monoterpenes while varying the speciation of NMVOC emissions from the solvent sector.

Table 2.3: The solvent sector emission inventories compared in this work.

Speciation	**Comment**	**Reference**
TNO	European average	Builtjes et al. (2002)
IPCC	Model Specific	Ehhalt et al. (2001)
EMEP	Model Specific	Simpson et al. (2012)
DE94	Country Specific	Friedrich et al. (2002)
GR95	Country Specific	Sidiropoulos and Tsilingiridis (2007)
GR05	Country Specific	Sidiropoulos and Tsilingiridis (2007)
UK98	Country Specific	Goodwin (2000)
UK08	Country Specific	Murrells et al. (2010)

The NMVOC emissions of the solvent sector were assigned to MCM v3.2 species based on the speciations of each emission inventory. Model simulations were repeated using MOZART-4 and RADM2 to investigate whether changing the chemical mechanism affected the differences in ozone concentrations between the solvent sector emission inventories.

The final study looked at the ozone-temperature relationship over central Europe and used the emissions of NMVOC from Benelux (Belgium, Netherlands and Luxembourg). The TNO_MACCIII emissions for the year 2011 were used as anthropogenic NMVOC emissions and mapped to MCM v3.2 species. Temperature indepedent emissions of biogenic species (isoprene and monoterpenes) were taken from the EMEP speciation (Simpson et al., 2012). Simulations using temperature-dependent emissions of isoprene used the MEGAN2.1 (Guenther et al., 2012) algorithm. All simulations were repeated using the CRI v2, MOZART-4, RADM2 and CB05 chemical mechanisms.

NO_x Initial Conditions

NO_x conditions generating VOC-and-NO_x sensitive chemistry were used in the first two studies. This was achieved by emitting the amount of NO required to balance the source of radicals at each time step. While the final study assessed the relationship between ozone and temperature with different NO_x conditions. For these simulations, a constant source of NO emissions was systematically varied between 5.0×10^9 and 1.5×10^{12} molecules (NO) cm^{-2} s^{-1} at each temperature used in this study (15–40 °C).

Boundary Conditions

No chemical boundary conditions were used in the first two studies as the experiments considered a contained box. In the final study, MECCA included a diurnal profile of the PBL with vertical mixing into the free troposphere using the PBL heights from the BAERLIN2014 campaign (Bonn et al., 2016). The boundary conditions for the free troposphere mixing ratios for O_3, CH_4 and CO were set to 50 ppbv, 1.8 ppmv and 116 ppbv respectively. These mixing ratios were taken from the 700 hPa height using the MATCH-MPIC chemical weather forecast data (`http://cwf.iass-potsdam.de/`) from March 21st.

Chapter 3

Presentation of Papers

This chapter outlines the main findings in each scientific paper published as part of this thesis. These publications addressed the research questions framed in Sect. 1.5 and are found in Chaps. 6–8.

3.1 Paper I: A comparison of chemical mechanisms using tagged ozone production potential (TOPP) analysis

Published: J. Coates and T. M. Butler. A comparison of chemical mechanisms using tagged ozone production potential (TOPP) analysis. *Atmospheric Chemistry and Physics*, 15(15):8795–8808, 2015.

The first paper presents a box modelling study where the effects on ozone production from VOC degradation chemistry in reduced chemical mechanisms (Table 2.2) was compared to the detailed MCM chemical mechanisms. Other chemical mechanism comparison studies noted differences in ozone levels between chemical mechanisms, however these studies did not deduce the root causes for these differences. This chemical mechanism comparison used the tagging approach described in Sect. 2.2.2 to give insights into how the simplified representation of VOC degradation by chemical mechanisms influenced ozone production.

The ozone production from the degradation of VOCs typical of urban environments were compared between the different chemical mechanisms. The box model simulated maximum ozone production (VOC-and-NO_x-sensitive) regime by

emitting the amount of NO required to balance the source of radicals at each time step. As described in Sect. 2.2.2, the tagging approach used the production of O_x as a proxy for ozone production.

The simulated ozone mixing ratios using reduced chemical mechanisms were generally lower than the ozone mixing ratios using the reference MCM chemical mechanisms on the first two days of simulations. Only the CRI v2 and RADM2 produced higher ozone mixing ratios than the MCM chemical mechanisms. Higher ozone mixing ratios using CRI v2 than the MCM were obtained during the development of the CRI v2. In RADM2, a lower yield of ketones from the degradation of HC3 (representing less-reactive VOC such as alkanes and alcohols) compared to the MCM led to higher ozone mixing ratios with RADM2.

The VOC degradation described in CRI v2, a lumped-intermediate chemical mechanism, produced the most similar amounts of O_x to the MCM v3.2 for each VOC. On the other hand, the degradation of VOC in all other reduced chemical mechanisms led to differences in O_x production with the largest differences occuring after the first day of simulations. The degradation of aromatic VOC in the reduced chemical mechanisms led to the largest differences in O_x production from the MCM v3.2.

Many VOC are broken down into smaller-sized degradation products faster on the first day in reduced chemical mechanisms than the MCM v3.2. The faster breakdown of VOC leads to lower amounts of larger-sized degradation products that can further degrade and produce O_x in the reduced chemical mechanisms. Thus, many VOC in reduced chemical mechanisms produce a lower maximum of O_x than the MCM v3.2 resulting in lower O_3 mixing ratios from the reduced chemical mechanisms compared to the MCM v3.2.

Reactive VOC, such as alkenes and aromatic VOC, produce maximum O_x on the first day of the simulations. Alkenes produce similar amounts of O_x on the first day between chemical mechanisms; differences in O_x production arise when mechanism species are used to represent individual VOC. Large inter-mechanism differences in O_x production result from the degradation of aromatic VOC on the first day due to the faster break down of the mechanism species representing aromatic VOC in reduced chemical mechanisms. The less-reactive alkanes produce maximum O_x on the second day of simulations and this maximum is lower in each reduced chemical mechanism than the MCM v3.2 due to the faster break down of alkanes into smaller sized degradation products on the first day.

3.2 Paper II: Variation of the NMVOC Speciation in the Solvent Sector and the Sensitivity of Modelled Tropospheric Ozone

Published: E. von Schneidemesser, J. Coates, A. J. H. Visschedijk, H. A. C. Denier van der Gon, and T. M. Butler. Variation of the NMVOC speciation in the solvent sector and the sensitivity of modelled tropospheric ozone. *Atmospheric Environment*, Submitted for Publication, 2016.

The second publication compared the ozone levels produced when using different emission inventories of NMVOC emissions for the solvent sector within a box model. Different chemical mechanisms (MCM v3.2, MOZART-4 and RADM2) were used to ascertain whether the representation of tropospheric chemistry affected the differences in ozone production when using the different emission inventories.

Emission inventories (EIs) are a critical model input but also a major source of uncertainty in modelling studies. For example, the speciations of EIs in many locations are not reflected by ambient measurements, EIs may not adequately reflect the temporal nature of emissions and many EIs may be outdated. Before taking upon the huge task of updating EIs addressing these issues, a scoping study looking at the sensitivity of ozone production when changing the model input from was performed in this study.

The experimental setup considered emissions from the solvent sector as this sector has the largest contribution to NMVOC. Model simulations used NO_x conditions simulating VOC-and-NO_x-sensitive conditions thus looking at the differences in maximum ozone production when using the emission inventories for the solvent sector in Table 2.3. Furthermore, simulations were performed using different chemical mechanisms (MCM v3.2, MOZART-4 and RADM2) comparing the differences with different representations of VOC degradation chemistry. Simulations using the tagging chemical mechanisms in Sect. 3.1 were performed allowing allocation of O_x production to the emitted NMVOC specified by each EI.

A maximum difference in ozone mixing ratios ranging between 11 ppb and 15 ppbv when using the different EIs was obtained from the box model simulations using each chemical mechanism. When using the same EI speciation, a maximum difference of 6.7 ppbv in ozone mixing ratios was determined between simulations with different chemical mechanisms. Thus both the choice of chemical mechanism and EI influenced the amount of ozone produced.

Further simulations using emissions from all other non-solvent sectors while varying the emissions from the solvent sector produced a lower maximum difference in ozone mixing ratio (6–9 ppbv) for each chemical mechanism. When further including emissions from biogenic sources reduced the maximum differences in ozone mixing ratios even further (5–8 ppbv) with each chemical mechanism.

Reactive VOC, such as alkenes and aromatic VOC, had the highest contribution to O_x production on the first day. While less-reactive VOC, such as alkanes and oxygenated VOC, contributed the most to the cumulative O_x production after seven days.

EIs specifying more emissions of alkanes produced more O_x than EIs specifying larger emissions from oxygenated NMVOC. A positive correlation between O_x production and the specification of alkane species by the EIs was determined while a negative correlation was determined between cumulative O_x production and specification of oxygenated species by the EIs. No correlation was found between the specification of aromatic species by EIs and O_x production and not all EIs specify alkene emissions thus no correlation was made between alkene emissions and O_x production.

3.3 Paper III: The Influence of Temperature on Ozone Production under varying NO_x Conditions – a modelling study

Published: J. Coates, K. A. Mar, and T. M. Butler. The influence of temperature on ozone production under varying NO_x conditions – a modelling study. *Atmospheric Chemistry and Physics Discussions*, In preparation, 2016.

The final study of this thesis looked at the ozone-temperature relationship with different NO_x conditions simulated by a box model. A non-linear relationship between ozone production with temperature and NO_x conditions has been noted using an analytical model constrained to observational measurements but not yet reproduced in a modelling study. Temperature increases ozone production through increasing NMVOC emissions from biogenic sources and by increasing the rates of chemical reactions. Modelling studies have as yet not quantified which of these effects is more important for ozone production. The study aimed to determine whether temperature-dependent increases in reaction rates or isoprene emissions were more important for ozone production on the urban scale and whether the non-linear

relationship of ozone with temperature and NO_x was reproduced using different chemical mechanisms.

Box model simulations were performed using NMVOC emissions representative of central Europe, first using a temperature-independent source of isoprene emissions followed by simulations using the temperature-dependent source of isoprene emissions described using the MEGAN2.1 algorithm. The choice of chemical mechanism may also influence the relationship of ozone on temperature, thus all simulations were repeated using the MCM v3.2, CRI v2, MOZART-4, RADM2 and CB05 chemical mechanisms. Model simulations were performed by systematically varying the temperature and NO emissions at each temperature (Sect. 2.3). The tagged chemical mechanisms could not be used in this study as the NO_x conditions gave rise to simulations with NO_x-saturated conditions where using O_x production as a proxy for ozone production is not valid (Sect. 2.2.2).

A non-linear relationship of ozone with temperature and NO_x emissions was produced using each chemical mechanism. This non-linear relationship was similar to that previously reported from observational studies. In each chemical mechanism, the absolute increase in ozone with temperature was greater for temperature-dependent chemistry than the increase ozone with temperature due to isoprene emissions. The largest increases in ozone mixing ratios were obtained in High-NO_x conditions and the lowest increase in ozone mixing ratios was achieved using Low-NO_x conditions.

Analysis of O_x production and consumption budgets showed that the net increase in O_x production with temperature was due to the faster reaction rates of initial oxidation of VOCs. The increase in OH with temperature, coupled to the increase of ozone with temperature, led to faster reaction rates of VOC oxidation with temperature.

Normalised production budgets of O_x with temperature were similar between chemical mechanisms. Thus the representations of VOC emissions by the chemical mechanisms led to differences in the ozone-temperature relationship between chemical mechanisms.

The box model results were also compared to observational data and output from the 3-D model WRF-Chem. The rate of increase of ozone with temperature from the box model was about half the rate of increase of ozone with temperature using observational and WRF-Chem output. The lack of sensitivity of the increase in ozone with temperature in the box model was due to focusing on instantaneous ozone production. Observational data and the output of 3-D models such as WRF-Chem include additional effects of temperature on ozone, such as stagnant conditions, where

high temperatures and low wind speeds lead to a build-up of ozone from previous days and these conditions were not considered in the experiments.

Chapter 4

Overall Discussion and Conclusions

Chapter 5

Summary and Zusammenfassung

References

J. Abbatt, C. George, M. Melamed, P. Monks, S. Pandis, and Y. Rudich. New directions: Fundamentals of atmospheric chemistry: Keeping a three-legged stool balanced. *Atmospheric Environment*, 84:390 – 391, 2014.

R. Atkinson. Atmospheric chemistry of VOCs and NO_x. *Atmospheric Environment*, 34(12-14):2063–2101, 2000.

A. Baklanov, K. Schlünzen, P. Suppan, J. Baldasano, D. Brunner, S. Aksoyoglu, G. Carmichael, J. Douros, J. Flemming, R. Forkel, S. Galmarini, M. Gauss, G. Grell, M. Hirtl, S. Joffre, O. Jorba, E. Kaas, M. Kaasik, G. Kallos, X. Kong, U. Korsholm, A. Kurganskiy, J. Kushta, U. Lohmann, A. Mahura, A. Manders-Groot, A. Maurizi, N. Moussiopoulos, S. T. Rao, N. Savage, C. Seigneur, R. S. Sokhi, E. Solazzo, S. Solomos, B. Sørensen, G. Tsegas, E. Vignati, B. Vogel, and Y. Zhang. Online coupled regional meteorology chemistry models in Europe: current status and prospects. *Atmospheric Chemistry and Physics*, 14(1):317–398, 2014.

C. Bloss, V. Wagner, M. E. Jenkin, R. Vollamer, W. J. Bloss, J. D. Lee, D. E. Heard, K. Wirtz, M. Martin-Reviejo, G. Rea, J. C. Wenger, and M. J. Pilling. Development of a detailed chemical mechanism (MCMv3.1) for the atmospheric oxidation of aromatic hydrocarbons. *Atmospheric Chemistry and Physics*, 5:641–664, 2005.

B. Bonn, E. von Schneidemesser, D. Andrich, J. Quedenau, H. Gerwig, A. Lüdecke, J. Kura, A. Pietsch, C. Ehlers, D. Klemp, C. Kofahl, R. Nothard, A. Kerschbaumer, W. Junkermann, R. Grote, T. Pohl, K. Weber, B. Lode, P. Schönberger, G. Churkina, T. M. Butler, and M. G. Lawrence. BAERLIN2014 - The influence of land surface types on and the horizontal heterogeneity of air pollutant levels in Berlin. *Atmospheric Chemistry and Physics Discussions*, 2016:1–62, 2016.

A. Boynard, A. Borbon, T. Leonardis, B. Barletta, S. Meinardi, D. R. Blake, and N. Locoge. Spatial and seasonal variability of measured anthropogenic non-methane hydrocarbons in urban atmospheres: Implication on emission ratios. *Atmospheric Environment*, 82(0):258–267, 2014.

P. Builtjes, M. Loon, M. Schaap, S. Teeuwisse, A. Visschedijk, and J. Bloos. The development of an emission data base over Europe and further contributions of TNO-MEP. Technical report, TNO Environment, 2002.

T. Butler, M. Lawrence, D. Taraborrelli, and J. Lelieveld. Multi-day ozone production potential of volatile organic compounds calculated with a tagging approach. *Atmospheric Environment*, 45(24):4082 – 4090, 2011.

T. M. Butler and M. G. Lawrence. The influence of megacities on global atmospheric chemistry: a modelling study. *Environmental Chemistry*, 6:219–225, 2009.

L. Camalier, W. Cox, and P. Dolwick. The effects of meteorology on ozone in urban areas and their use in assessing ozone trends. *Atmospheric Environment*, 41(33):7127 – 7137, 2007.

W. P. Carter. Development of ozone reactivity scales for volatile organic compounds. *Air & Waste*, 44(7):881–899, 1994.

W. P. L. Carter. Development of a Database for Chemical Mechanism Assignments for Volatile Organic Emissions. *Journal of the Air & Waste Management Association*, 0, 2015.

J. Coates and T. M. Butler. A comparison of chemical mechanisms using tagged ozone production potential (TOPP) analysis. *Atmospheric Chemistry and Physics*, 15(15):8795–8808, 2015.

J. Coates, K. A. Mar, and T. M. Butler. The influence of temperature on ozone production under varying NO_x conditions – a modelling study. *Atmospheric Chemistry and Physics Discussions*, In preparation, 2016.

I. Coll, C. Rousseau, B. Barletta, S. Meinardi, and D. R. Blake. Evaluation of an urban NMHC emission inventory by measurements and impact on CTM results. *Atmospheric Environment*, 44(31):3843 – 3855, 2010.

A. C. Comrie. Comparing neural networks and regression models for ozone forecasting. *Journal of the Air & Waste Management Association*, 47(6):653–663, 1997.

G. Curci, M. Beekmann, R. Vautard, G. Smiatek, R. Steinbrecher, J. Theloke, and R. Friedrich. Modelling study of the impact of isoprene and terpene biogenic emissions on European ozone levels. *Atmospheric Environment*, 43(7):1444 – 1455, 2009.

V. Damian, A. Sandu, M. Damian, F. Potra, and G. R. Carmichael. The kinetic preprocessor KPP-a software environment for solving chemical kinetics. *Computers & Chemical Engineering*, 26(11):1567 – 1579, 2002.

J. P. Dawson, P. J. Adams, and S. N. Pandis. Sensitivity of ozone to summertime climate in the eastern USA: A modeling case study . *Atmospheric Environment*, 41 (7):1494 – 1511, 2007.

H. Denier van der Gon, C. Hendriks, J. Kuenen, A. Segers, and A. Visschedijk. Description of current temporal emission patterns and sensitivity of predicted AQ for temporal emission patterns. Technical Report EU FP7 MACC report: D_D-EMIS_1.3, TNO, 2011.

R. M. Doherty, O. Wild, D. T. Shindell, G. Zeng, I. A. MacKenzie, W. J. Collins, A. M. Fiore, D. S. Stevenson, F. J. Dentener, M. G. Schultz, P. Hess, R. G. Derwent, and T. J. Keating. Impacts of climate change on surface ozone and intercontinental ozone pollution: A multi-model study. *Journal of Geophysical Research: Atmospheres*, 118(9):3744–3763, 2013.

C. Dueñas, M. Fernández, S. Cañete, J. Carretero, and E. Liger. Assessment of ozone variations and meteorological effects in an urban area in the Mediterranean Coast. *Science of The Total Environment*, 299(1–3):97 – 113, 2002.

EEA. Air quality in Europe - 2011 report. Technical Report 12/2011, European Environmental Agency, 2011.

EEA. Air quality in Europe - 2013 report. Technical Report 9/2013, European Environmental Agency, 2013.

EEA. Air quality in Europe - 2015 report. Technical Report 5/2015, European Environmental Agency, 2015.

Ehhalt, D., Prather, M., Dentener, F., Derwent, R., Dlugokencky, E., Holland, E., Isaksen, I., Katima, J., Kirchhoff, V., Matson, P., Midgley, P., Wang, and M. Climate Change 2001: The Scientific Basis. Contribution of Working Group I to the Third Assessment Report of the Intergovernmental Panel on Climate Change. Technical report, IPCC, 2001.

K. M. Emmerson and M. J. Evans. Comparison of tropospheric gas-phase chemistry schemes for use within global models. *Atmospheric Chemistry and Physics*, 9(5): 1831–1845, 2009.

L. K. Emmons, S. Walters, P. G. Hess, J.-F. Lamarque, G. G. Pfister, D. Fillmore, C. Granier, A. Guenther, D. Kinnison, T. Laepple, J. Orlando, X. Tie, G. Tyndall, C. Wiedinmyer, S. L. Baughcum, and S. Kloster. Description and evaluation of the Model for Ozone and Related chemical Tracers, version 4 (MOZART-4). *Geoscientific Model Development*, 3(1):43–67, 2010.

L. K. Emmons, P. G. Hess, J.-F. Lamarque, and G. G. Pfister. Tagged ozone mechanism for mozart-4, cam-chem and other chemical transport models. *Geoscientific Model Development*, 5(6):1531–1542, 2012.

V. Eyring, J.-F. Lamarque, P. Hess, F. Arfeuille, K. Bowman, M. P. Chipperfield, B. Duncan, A. Fiore, A. Gettelman, M. A. Giorgetta, C. Granier, M. Hegglin, D. Kinnison, M. Kunze, U. Langematz, B. Luo, R. Martin, K. Matthes, P. A. Newman, T. Peter, A. Robock, T. Ryerson, A. Saiz-Lopez, R. Salawitch, M. Schultz, T. G. Shepherd, D. Shindell, J. Staehelin, S. Tegtmeier, L. Thomason, S. Tilmes, J.-P. Vernier, D. W. Waugh, , and P. J. Young. Overview of IGAC/SPARC Chemistry-Climate Model Initiative (CCMI) Community Simulations in Support of Upcoming Ozone and Climate Assessments. *SPARC Newsletter*, 40:48–66, 2013.

R. Friedrich, B. Wickert, P. Blank, S. Emeis, W. Engewald, D. Hassel, H. Hoffmann, H. Michael, A. Obermeier, K. Schäfer, T. Schmitz, A. Sedlmaier, M. Stockhause, J. Theloke, and F.-J. Weber. Development of Emission Models and Improvement of Emission Data for Germany. *Journal of Atmospheric Chemistry*, 42(1):179–206, 2002.

M. W. Gery, G. Z. Whitten, J. P. Killus, and M. C. Dodge. A photochemical kinetics mechanism for urban and regional scale computer modeling. *Journal of Geophysical Research*, 94(D10):12,925–12,956, 1989.

W. S. Goliff, W. R. Stockwell, and C. V. Lawson. The regional atmospheric chemistry mechanism, version 2. *Atmospheric Environment*, 68:174 – 185, 2013.

J. Goodwin. UK Emissions of Air Pollutants 1970 to 1998. Technical report, DEFRA, 2000.

G. Grell, S. Peckham, R. Schmitz, S. McKeen, G. Frost, W. Skamarock, and B. Eder. Fully coupled "online" chemistry within the WRF model. *Atmospheric Environment*, 39(37):6957–6975, 2005.

S. Grice, J. Stedman, A. Kent, M. Hobson, J. Norris, J. Abbott, and S. Cooke. Recent trends and projections of primary NO2 emissions in Europe. *Atmospheric Environment*, 43(13):2154 – 2167, 2009.

A. Guenther, T. Karl, P. Harley, C. Wiedinmyer, P. I. Palmer, and C. Geron. Estimates of global terrestrial isoprene emissions using MEGAN (Model of Emissions of Gases and Aerosols from Nature). *Atmospheric Chemistry and Physics*, 6(11): 3181–3210, 2006.

A. B. Guenther, X. Jiang, C. L. Heald, T. Sakulyanontvittaya, T. Duhl, L. K. Emmons, and X. Wang. The Model of Emissions of Gases and Aerosols from Nature version 2.1 (MEGAN2.1): an extended and updated framework for modeling biogenic emissions. *Geoscientific Model Development*, 5(6):1471–1492, 2012.

D. W. Gunz and M. R. Hoffmann. Atmospheric chemistry of peroxides: a review. *Atmospheric Environment. Part A. General Topics*, 24(7):1601 – 1633, 1990.

D. A. Hauglustaine, G. P. Brasseur, S. Walters, P. J. Rasch, J.-F. Müller, L. K. Emmons, and M. A. Carroll. MOZART, a global chemical transport model for ozone and related chemical tracers 2. Model results and evaluation. *Journal of Geophysical Research*, 103(D21):28,291–28,335, 1998.

IARC. Outdoor air pollution a leading environmental cause of cancer deaths. `https://www.iarc.fr/en/media-centre/iarcnews/pdf/pr221_E.pdf`, 2013. [Online; accessed 31-December-2015].

D. J. Jacob and D. A. Winner. Effect of climate change on air quality. *Atmospheric Environment*, 43(1):51 – 63, 2009. Atmospheric Environment - Fifty Years of Endeavour.

M. Jenkin, L. Watson, S. Utembe, and D. Shallcross. A Common Representative Intermediates (CRI) mechanism for VOC degradation. Part 1: Gas phase mechanism development. *Atmospheric Environment*, 42(31):7185 – 7195, 2008.

M. E. Jenkin and K. C. Clemitshaw. Ozone and other secondary photochemical pollutants: Chemical processes governing their formation in the planetary boundary layer. *Atmospheric Environment*, 34(16):2499–2527, 2000.

M. E. Jenkin, S. M. Saunders, and M. J. Pilling. The tropospheric degradation of volatile organic compounds: a protocol for mechanism development. *Atmospheric Environment*, 31(1):81 – 104, 1997.

M. E. Jenkin, S. M. Saunders, V. Wagner, and M. J. Pilling. Protocol for the development of the Master Chemical Mechanism, MCM v3 (Part B): tropospheric degradation of aromatic volatile organic compounds. *Atmospheric Chemistry and Physics*, 3(1):181–193, 2003.

S. Kirschke, P. Bousquet, P. Ciais, M. Saunois, J. G. Canadell, E. J. Dlugokencky, P. Bergamaschi, D. Bergmann, D. R. Blake, L. Bruhwiler, P. Cameron-Smith, S. Castaldi, F. Chevallier, L. Feng, A. Fraser, M. Heimann, E. L. Hodson, S. Houweling, B. Josse, P. J. Fraser, P. B. Krummel, J.-F. Lamarque, R. L. Langenfelds, C. Le Quere, V. Naik, S. O'Doherty, P. I. Palmer, I. Pison, D. Plummer,

B. Poulter, R. G. Prinn, M. Rigby, B. Ringeval, M. Santini, M. Schmidt, D. T. Shindell, I. J. Simpson, R. Spahni, L. P. Steele, S. A. Strode, K. Sudo, S. Szopa, G. R. van der Werf, A. Voulgarakis, M. van Weele, R. F. Weiss, J. E. Williams, and G. Zeng. Three decades of global methane sources and sinks. *Nature Geoscience*, 6 (10):813–823, 2013.

L. I. Kleinman. Low and high NO_x tropospheric photochemistry. *Journal of Geophysical Research*, 99(D8):16,831–16,838, 1994.

D. Kubistin, H. Harder, M. Martinez, M. Rudolf, R. Sander, H. Bozem, G. Eerdekens, H. Fischer, C. Gurk, T. Klüpfel, R. Königstedt, U. Parchatka, C. L. Schiller, A. Stickler, D. Taraborrelli, J. Williams, and J. Lelieveld. Hydroxyl radicals in the tropical troposphere over the Suriname rainforest: comparison of measurements with the box model MECCA. *Atmospheric Chemistry and Physics*, 10(19):9705–9728, 2010.

J. J. P. Kuenen, A. J. H. Visschedijk, M. Jozwicka, and H. A. C. Denier van der Gon. TNO-MACC_II emission inventory; a multi-year (2003–2009) consistent high-resolution european emission inventory for air quality modelling. *Atmospheric Chemistry and Physics*, 14(20):10963–10976, 2014.

M. Kuhn, P. Builtjes, D. Poppe, D. Simpson, W. Stockwell, Y. Andersson-Sko¨ld, A. Baart, M. Das, F. Fiedler, Ø. Hov, F. Kirchner, P. Makar, J. Milford, M. Roemer, R. Ruhnke, A. Strand, B. Vogel, and H. Vogel. Intercomparison of the gas-phase chemistry in several chemistry and transport models. *Atmospheric Environment*, 32 (4):693 – 709, 1998.

J.-F. Lamarque, T. C. Bond, V. Eyring, C. Granier, A. Heil, Z. Klimont, D. Lee, C. Liousse, A. Mieville, B. Owen, M. G. Schultz, D. Shindell, S. J. Smith, E. Stehfest, J. Van Aardenne, O. R. Cooper, M. Kainuma, N. Mahowald, J. R. McConnell, V. Naik, K. Riahi, and D. P. van Vuuren. Historical (1850–2000) gridded anthropogenic and biomass burning emissions of reactive gases and aerosols: methodology and application. *Atmospheric Chemistry and Physics*, 10(15):7017–7039, 2010.

J. Lelieveld and F. J. Dentener. What controls tropospheric ozone? *Journal of Geophysical Research: Atmospheres*, 105(D3):3531–3551, 2000.

A. S. M. Lourens, T. M. Butler, J. P. Beukes, P. G. van Zyl, G. D. Fourie, and M. G. Lawrence. Investigating atmospheric photochemistry in the Johennesburg-Pretoria megacity using a box model. *South African Journal of Science*, 112(1/2), 2016.

P. S. Monks. A review of the observations and origins of the spring ozone maximum. *Atmospheric Environment*, 34(21):3545 – 3561, 2000.

P. S. Monks. Gas-phase radical chemistry in the troposphere. *Chem. Soc. Rev.*, 34: 376–395, 2005.

T. P. Murrells, N.R.P., G. Thistlethwaite, A. Wagner, Y. Li, T.B., J. Norris, C. Walker, R. A. Stewart, I. Tsagatakis, R. Whiting, C.C., S. Okamura, M. Peirce, S. Sneddon, J. Webb, J.T., J. MacCarthy, S. Choudrie, and N. Brophy. UK Emissions of Air Pollutants 1970 to 2008. Technical report, DEFRA, Didcot, UK, 2010.

J. Olivier, J. Berdowski, J. Bakker, A. Visschedijk, and J. Bloos. Applications of EDGAR. Including a description of EDGAR 3.0: reference database with trend data for 1970–1995. Technical Report RIVM report No. 773301 001/NOP report no. 410200 051, RIVM, 2001.

N. Otero, J. Sillmann, J. L. Schnell, H. W. Rust, and T. Butler. Synoptic and meteorological drivers of extreme ozone concentrations over europe. *Environmental Research Letters*, 11(2):024005, 2016.

S. A. Penkett and K. A. Brice. The spring maximum of photo-oxidants in the Northern Hemisphere troposphere. *Nature*, 319:655–657, 1986.

S. E. Pusede, D. R. Gentner, P. J. Wooldridge, E. C. Browne, A. W. Rollins, K.-E. Min, A. R. Russell, J. Thomas, L. Zhang, W. H. Brune, S. B. Henry, J. P. DiGangi, F. N. Keutsch, S. A. Harrold, J. A. Thornton, M. R. Beaver, J. M. St. Clair, P. O. Wennberg, J. Sanders, X. Ren, T. C. VandenBoer, M. Z. Markovic, A. Guha, R. Weber, A. H. Goldstein, and R. C. Cohen. On the temperature dependence of organic reactivity, nitrogen oxides, ozone production, and the impact of emission controls in San Joaquin Valley, California. *Atmospheric Chemistry and Physics*, 14 (7):3373–3395, 2014.

S. E. Pusede, A. L. Steiner, and R. C. Cohen. Temperature and Recent Trends in the Chemistry of Continental Surface Ozone. *Chemical Reviews*, 115(10):3898–3918, 2015.

A. Rickard, J. Young, M. J. Pilling, M. E. Jenkin, S. Pascoe, and S. M. Saunders. The Master Chemical Mechanism Version MCM v3.2. `http://mcm.leeds.ac.uk/MCMv3.2/`, 2015. [Online; accessed 25-March-2015].

A. Russell and R. Dennis. NARSTO critical review of photochemical models and modeling. *Atmospheric Environment*, 34(12–14):2283 – 2324, 2000.

R. Sander, A. Kerkweg, P. Jöckel, and J. Lelieveld. Technical note: The new comprehensive atmospheric chemistry module mecca. *Atmospheric Chemistry and Physics*, 5(2):445–450, 2005.

S. M. Saunders, M. E. Jenkin, R. G. Derwent, and M. J. Pilling. Protocol for the development of the Master Chemical Mechanism, MCM v3 (Part A): tropospheric degradation of non-aromatic volatile organic compounds. *Atmospheric Chemistry and Physics*, 3(1):161–180, 2003.

J. H. Seinfeld and S. N. Pandis. *Atmospheric Chemistry and Physics: From Air Pollution to Climate Change*. John Wiley & Sons Inc, New York, second edition, 2006.

C. Sidiropoulos and G. Tsilingiridis. Composition changes of NMVOC emissions from solvent use in Greece for the period 1990-2005. *Fresenius Environmental Bulletin*, 16(9):1108–1112, 2007.

S. Sillman and P. J. Samson. Impact of temperature on oxidant photochemistry in urban, polluted rural and remote environments. *Journal of Geophysical Research: Atmospheres*, 100(D6):11497–11508, 1995.

D. Simpson, A. Benedictow, H. Berge, R. Bergström, L. D. Emberson, H. Fagerli, C. R. Flechard, G. D. Hayman, M. Gauss, J. E. Jonson, M. E. Jenkin, A. Nyíri, C. Richter, V. S. Semeena, S. Tsyro, J.-P. Tuovinen, Á. Valdebenito, and P. Wind. The EMEP MSC-W chemical transport model – technical description. *Atmospheric Chemistry and Physics*, 12(16):7825–7865, 2012.

W. R. Stockwell, P. Middleton, J. S. Chang, and X. Tang. The second generation regional acid deposition model chemical mechanism for regional air quality modeling. *Journal of Geophysical Research: Atmospheres*, 95(D10):16343–16367, 1990.

W. R. Stockwell, F. Kirchner, M. Kuhn, and S. Seefeld. A new mechanism for regional atmospheric chemistry modeling. *Journal of Geophysical Research: Atmospheres*, 102(D22):25847–25879, 1997.

W. R. Stockwell, C. V. Lawson, E. Saunders, and W. S. Goliff. A review of tropospheric atmospheric chemistry and gas-phase chemical mechanisms for air quality modeling. *Atmosphere*, 3(1):1, 2012.

S. Syri, M. Amann, W. Schöpp, and C. Heyes. Estimating long-term population exposure to ozone in urban areas of Europe. *Environmental Pollution*, 113(1):59 – 69, 2001.

E. von Schneidemesser, P. S. Monks, V. Gros, J. Gauduin, and O. Sanchez. How important is biogenic isoprene in an urban environment? a study in london and paris. *Geophysical Research Letters*, 38(19), 2011. L19804.

E. von Schneidemesser, P. S. Monks, J. D. Allan, L. Bruhwiler, P. Forster, D. Fowler, A. Lauer, W. T. Morgan, P. Paasonen, M. Righi, K. Sindelarova, and M. A. Sutton. Chemistry and the Linkages between Air Quality and Climate Change. *Chemical Reviews*, 2015. PMID: 25926133.

E. von Schneidemesser, J. Coates, A. J. H. Visschedijk, H. A. C. Denier van der Gon, and T. M. Butler. Variation of the NMVOC speciation in the solvent sector and the sensitivity of modelled tropospheric ozone. *Atmospheric Environment*, Submitted for Publication, 2016.

World Meteorological Organisation. Scientific Assessment of Ozone Depletion: 2010. Technical Report 516 pp., World Meteorological Organisation, Geneva, Switzerland, March 2011.

G. Yarwood, S. Rao, M. Yocke, and G. Z. Whitten. Updates to the Carbon Bond Chemical Mechanism: CB05. Technical report, U. S Environmental Protection Agency, 2005.

P. J. Young, A. T. Archibald, K. W. Bowman, J.-F. Lamarque, V. Naik, D. S. Stevenson, S. Tilmes, A. Voulgarakis, O. Wild, D. Bergmann, P. Cameron-Smith, I. Cionni, W. J. Collins, S. B. Dalsøren, R. M. Doherty, V. Eyring, G. Faluvegi, L. W. Horowitz, B. Josse, Y. H. Lee, I. A. MacKenzie, T. Nagashima, D. A. Plummer, M. Righi, S. T. Rumbold, R. B. Skeie, D. T. Shindell, S. A. Strode, K. Sudo, S. Szopa, and G. Zeng. Pre-industrial to end 21st century projections of tropospheric ozone from the Atmospheric Chemistry and Climate Model Intercomparison Project (ACCMIP). *Atmospheric Chemistry and Physics*, 13(4):2063–2090, 2013.

Chapter 6

Paper 1: A comparison of chemical mechanisms using tagged ozone production potential (TOPP) analysis

Atmos. Chem. Phys., 15, 8795–8808, 2015
www.atmos-chem-phys.net/15/8795/2015/
doi:10.5194/acp-15-8795-2015

Atmospheric Chemistry and Physics Open Access

A comparison of chemical mechanisms using tagged ozone production potential (TOPP) analysis

J. Coates and T. M. Butler

Institute for Advanced Sustainability Studies, Potsdam, Germany

Correspondence to: J. Coates (jane.coates@iass-potsdam.de)

Received: 10 April 2015 – Published in Atmos. Chem. Phys. Discuss.: 29 April 2015
Revised: 23 July 2015 – Accepted: 24 July 2015 – Published: 10 August 2015

Abstract. Ground-level ozone is a secondary pollutant produced photochemically from reactions of NO_x with peroxy radicals produced during volatile organic compound (VOC) degradation. Chemical transport models use simplified representations of this complex gas-phase chemistry to predict O_3 levels and inform emission control strategies. Accurate representation of O_3 production chemistry is vital for effective prediction. In this study, VOC degradation chemistry in simplified mechanisms is compared to that in the near-explicit Master Chemical Mechanism (MCM) using a box model and by "tagging" all organic degradation products over multi-day runs, thus calculating the tagged ozone production potential (TOPP) for a selection of VOCs representative of urban air masses. Simplified mechanisms that aggregate VOC degradation products instead of aggregating emitted VOCs produce comparable amounts of O_3 from VOC degradation to the MCM. First-day TOPP values are similar across mechanisms for most VOCs, with larger discrepancies arising over the course of the model run. Aromatic and unsaturated aliphatic VOCs have the largest inter-mechanism differences on the first day, while alkanes show largest differences on the second day. Simplified mechanisms break VOCs down into smaller-sized degradation products on the first day faster than the MCM, impacting the total amount of O_3 produced on subsequent days due to secondary chemistry.

1 Introduction

Ground-level ozone (O_3) is both an air pollutant and a climate forcer that is detrimental to human health and crop growth (Stevenson et al., 2013). O_3 is produced from the reactions of volatile organic compounds (VOCs) and nitrogen oxides ($NO_x = NO + NO_2$) in the presence of sunlight (Atkinson, 2000).

Background O_3 concentrations have increased during the last several decades due to the increase of overall global anthropogenic emissions of O_3 precursors (HTAP, 2010). Despite decreases in emissions of O_3 precursors over Europe since 1990, EEA (2014) reports that 98 % of Europe's urban population are exposed to levels exceeding the WHO air quality guideline of 100 $\mu g\,m^{-3}$ over an 8 h mean. These exceedances result from local and regional O_3 precursor gas emissions, their intercontinental transport and the non-linear relationship of O_3 concentrations to NO_x and VOC levels (EEA, 2014).

Effective strategies for emission reductions rely on accurate predictions of O_3 concentrations using chemical transport models (CTMs). These predictions require adequate representation of gas-phase chemistry in the chemical mechanism used by the CTM. For reasons of computational efficiency, the chemical mechanisms used by global and regional CTMs must be simpler than the nearly explicit mechanisms which can be used in box modelling studies. This study compares the impacts of different simplification approaches of chemical mechanisms on O_3 production chemistry focusing on the role of VOC degradation products.

$$NO + O_3 \rightarrow NO_2 + O_2 \quad \text{(R1)}$$

$$NO_2 + h\nu \rightarrow NO + O(^3P) \quad \text{(R2)}$$

$$O_2 + O(^3P) + M \rightarrow O_3 + M \quad \text{(R3)}$$

The photochemical cycle (Reactions R1–R3) rapidly produces and destroys O_3. NO and NO_2 reach a near-steady state via Reactions (R1) and (R2) which is disturbed in two cases. Firstly, via O_3 removal (deposition or Reaction R1 during night-time and near large NO sources) and secondly,

when O_3 is produced through VOC–NO_x chemistry (Sillman, 1999).

VOCs (RH) are mainly oxidised in the troposphere by the hydroxyl radical (OH) forming peroxy radicals (RO_2) in the presence of O_2. For example, Reaction (R4) describes the OH oxidation of alkanes proceeding though abstraction of an H from the alkane. In high-NO_x conditions, typical of urban environments, RO_2 react with NO (Reaction R5) to form alkoxy radicals (RO), which react quickly with O_2 (Reaction R6) producing a hydroperoxy radical (HO_2) and a carbonyl species (R′CHO). The secondary chemistry of these first-generation carbon-containing oxidation products is analogous to the sequence of Reactions (R4–R6), producing further HO_2 and RO_2 radicals. Subsequent-generation oxidation products can continue to react, producing HO_2 and RO_2 until they have been completely oxidised to CO_2 and H_2O. Both RO_2 and HO_2 react with NO to produce NO_2 (Reactions R5 and R7) leading to O_3 production via Reactions (R2) and (R3). Thus, the amount of O_3 produced from VOC degradation is related to the number of NO to NO_2 conversions by RO_2 and HO_2 radicals formed during VOC degradation (Atkinson, 2000).

$$RH + OH + O_2 \rightarrow RO_2 + H_2O \quad \text{(R4)}$$

$$RO_2 + NO \rightarrow RO + NO_2 \quad \text{(R5)}$$

$$RO + O_2 \rightarrow R'CHO + HO_2 \quad \text{(R6)}$$

$$HO_2 + NO \rightarrow OH + NO_2 \quad \text{(R7)}$$

Three atmospheric regimes with respect to O_3 production can be defined (Jenkin and Clemitshaw, 2000). In the NO_x-sensitive regime, VOC concentrations are much higher than those of NO_x, and O_3 production depends on NO_x concentrations. On the other hand, when NO_x concentrations are much higher than those of VOCs (VOC-sensitive regime), VOC concentrations determine the amount of O_3 produced. Finally, the NO_x–VOC-sensitive regime produces maximal O_3 and is controlled by both VOC and NO_x concentrations.

These atmospheric regimes remove radicals through distinct mechanisms (Kleinman, 1991). In the NO_x-sensitive regime, radical concentrations are high relative to NO_x leading to radical removal by radical combination (Reaction R8) and bimolecular destruction (Reaction R9) (Kleinman, 1994).

$$RO_2 + HO_2 \rightarrow ROOH + O_2 \quad \text{(R8)}$$

$$HO_2 + OH \rightarrow H_2O + O_2 \quad \text{(R9)}$$

However, in the VOC-sensitive regime, radicals are removed by reacting with NO_2 leading to nitric acid (HNO_3) (Reaction R10) and PAN species (Reaction R11).

$$NO_2 + OH \rightarrow HNO_3 \quad \text{(R10)}$$

$$RC(O)O_2 + NO_2 \rightarrow RC(O)O_2NO_2 \quad \text{(R11)}$$

The NO_x–VOC-sensitive regime has no dominant radical removal mechanism as radical and NO_x amounts are comparable. This chemistry results in O_3 concentrations being a non-linear function of NO_x and VOC concentrations.

Individual VOCs impact O_3 production differently through their diverse reaction rates and degradation pathways. These impacts can be quantified using ozone production potentials (OPPs), which can be calculated through incremental reactivity (IR) studies using photochemical models. In IR studies, VOC concentrations are changed by a known increment and the change in O_3 production is compared to that of a standard VOC mixture. Examples of IR scales are the maximum incremental reactivity (MIR) and maximum ozone incremental reactivity (MOIR) scales in Carter (1994), as well as the photochemical ozone creation potential (POCP) scale of Derwent et al. (1996, 1998). The MIR, MOIR and POCP scales were calculated under different NO_x conditions, thus calculating OPPs in different atmospheric regimes.

Butler et al. (2011) calculate the maximum potential of a number of VOCs to produce O_3 by using NO_x conditions inducing NO_x–VOC-sensitive chemistry over multi-day scenarios using a "tagging" approach – the tagged ozone production potential (TOPP). Tagging involves labelling all organic degradation products produced during VOC degradation with the name of the emitted VOCs. Tagging enables the attribution of O_3 production from VOC degradation products back to the emitted VOCs, thus providing detailed insight into VOC degradation chemistry. Butler et al. (2011), using a near-explicit chemical mechanism, showed that some VOCs, such as alkanes, produce maximum O_3 on the second day of the model run; in contrast to unsaturated aliphatic and aromatic VOCs which produce maximum O_3 on the first day. In this study, the tagging approach of Butler et al. (2011) is applied to several chemical mechanisms of reduced complexity, using conditions of maximum O_3 production (NO_x–VOC-sensitive regime), to compare the effects of different representations of VOC degradation chemistry on O_3 production in the different chemical mechanisms.

A near-explicit mechanism, such as the Master Chemical Mechanism (MCM) (Jenkin et al., 2003; Saunders et al., 2003; Bloss et al., 2005), includes detailed degradation chemistry making the MCM ideal as a reference for comparing chemical mechanisms. Reduced mechanisms generally take two approaches to simplifying the representation of VOC degradation chemistry: lumped-structure approaches and lumped-molecule approaches (Dodge, 2000).

Lumped-structure mechanisms speciate VOCs by the carbon bonds of the emitted VOCs (e.g. the Carbon Bond mechanisms, CBM-IV (Gery et al., 1989) and CB05 (Yarwood et al., 2005)). Lumped-molecule mechanisms represent VOCs explicitly or by aggregating (lumping) many VOCs into a single mechanism species. Mechanism species may lump VOCs by functionality (MOdel for Ozone and Related chemical Tracers, MOZART-4, Emmons et al., 2010) or OH reactivity (Regional Acid Deposition Model, RADM2 (Stockwell et al., 1990), Regional Atmospheric Chemistry

Mechanism, RACM (Stockwell et al., 1997) and RACM2 (Goliff et al., 2013)). The Common Representative Intermediates mechanism (CRI) lumps the degradation products of VOCs rather than the emitted VOCs (Jenkin et al., 2008).

Many comparison studies of chemical mechanisms consider modelled time series of O_3 concentrations over varying VOC and NO_x concentrations. Examples are Dunker et al. (1984), Kuhn et al. (1998) and Emmerson and Evans (2009). The largest discrepancies between the time series of O_3 concentrations in different mechanisms from these studies arise when modelling urban rather than rural conditions and are attributed to the treatment of radical production, organic nitrate and night-time chemistry. Emmerson and Evans (2009) also compare the inorganic gas-phase chemistry of different chemical mechanisms; differences in inorganic chemistry arise from inconsistencies between IUPAC and JPL reaction rate constants.

Mechanisms have also been compared using OPP scales. OPPs are a useful comparison tool as they relate O_3 production to a single value. Derwent et al. (2010) compared the near-explicit MCM v3.1 and SAPRC-07 mechanisms using first-day POCP values calculated under VOC-sensitive conditions. The POCP values were comparable between the mechanisms. Butler et al. (2011) compared first-day TOPP values to the corresponding published MIR, MOIR and POCP values. TOPP values were most comparable to MOIR and POCP values due to the similarity of the chemical regimes used in their calculation.

In this study, we compare TOPP values of VOCs using a number of mechanisms to those calculated with the MCM v3.2, under standardised conditions which maximise O_3 production. Differences in O_3 production are explained by the differing treatments of secondary VOC degradation in these mechanisms.

2 Methodology

2.1 Chemical mechanisms

The nine chemical mechanisms compared in this study are outlined in Table 1 with a brief summary below. We used a subset of each chemical mechanism containing all the reactions needed to fully describe the degradation of the VOCs in Table 2. The reduced mechanisms in this study were chosen as they are commonly used in 3-D models and apply different approaches to representing secondary VOC chemistry. The recent review by Baklanov et al. (2014) shows that each chemical mechanism used in this study are actively used by modelling groups.

The MCM (Jenkin et al., 1997, 2003; Saunders et al., 2003; Bloss et al., 2005; Rickard et al., 2015) is a near-explicit mechanism which describes the degradation of 125 primary VOCs. The MCM v3.2 is the reference mechanism in this study due to its level of detail (16 349 organic reactions). Despite this level of detail, the MCM had difficulties in reproducing the results of chamber study experiments involving aromatic VOCs (Bloss et al., 2005).

The CRI (Jenkin et al., 2008) is a reduced chemical mechanism with 1145 organic reactions describing the oxidation of the same primary VOCs as the MCM v3.1 (12 691 organic reactions). VOC degradation in the CRI is simplified by lumping the degradation products of many VOCs into mechanism species whose overall O_3 production reflects that of the MCM v3.1. The CRI v2 is available in more than one reduced variant, described in Watson et al. (2008). We used a subset of the full version of the CRI v2 (http://mcm.leeds.ac.uk/CRI). Differences in O_3 production between the CRI v2 and MCM v3.2 may be due to changes in the MCM versions rather than the CRI reduction techniques, hence the MCM v3.1 is also included in this study.

MOZART-4 represents global tropospheric and stratospheric chemistry (Emmons et al., 2010). Explicit species exist for methane, ethane, propane, ethene, propene, isoprene and α-pinene. All other VOCs are represented by lumped species determined by the functionality of the VOCs. Tropospheric chemistry is described by 145 organic reactions in MOZART-4.

RADM2 (Stockwell et al., 1990) describes regional-scale atmospheric chemistry using 145 organic reactions with explicit species representing methane, ethane, ethene and isoprene. All other VOCs are assigned to lumped species based on OH reactivity and molecular weight. RADM2 was updated to RACM (Stockwell et al., 1997) with more explicit and lumped species representing VOCs as well as revised chemistry (193 organic reactions). RACM2 is the updated RACM version (Goliff et al., 2013) with substantial updates to the chemistry, including more lumped and explicit species representing emitted VOCs (315 organic reactions).

CBM-IV (Gery et al., 1989) uses 46 organic reactions to simulate polluted urban conditions and represents ethene, formaldehyde and isoprene explicitly while all other emitted VOCs are lumped by their carbon bond types. All primary VOCs were assigned to lumped species in CBM-IV as described in Hogo and Gery (1989). For example, the mechanism species PAR represents the C–C bond. Pentane, having five carbon atoms, is represented as 5 PAR. A pentane mixing ratio of 1200 pptv is assigned to 6000 ($= 1200 \times 5$) pptv of PAR in CBM-IV. CBM-IV was updated to CB05 (Yarwood et al., 2005) by including further explicit species representing methane, ethane and acetaldehyde, and has 99 organic reactions. Other updates include revised allocation of primary VOCs and updated rate constants.

2.2 Model set-up

The modelling approach and set-up follows the original TOPP study of Butler et al. (2011). The approach is summarised here; further details can be found in the Supplement and in Butler et al. (2011). We use the MECCA box model,

Table 1. The chemical mechanisms used in the study are shown here. MCM v3.2 is the reference mechanism. The number of organic species and reactions needed to fully oxidise the VOCs in Table 2 for each mechanism are also included.

Chemical mechanism	Number of organic species	Number of organic reactions	Type of lumping	Reference	Recent study
MCM v3.2	1884	5621	No lumping	Rickard et al. (2015)	Koss et al. (2015)
MCM v3.1	1677	4862	No lumping	Jenkin et al. (1997) Saunders et al. (2003) Jenkin et al. (2003) Bloss et al. (2005)	Lidster et al. (2014)
CRI v2	189	559	Lumped intermediates	Jenkin et al. (2008)	Derwent et al. (2015)
MOZART-4	61	135	Lumped molecule	Emmons et al. (2010)	Hou et al. (2015)
RADM2	42	105	Lumped molecule	Stockwell et al. (1990)	Li et al. (2014)
RACM	51	152	Lumped molecule	Stockwell et al. (1997)	Ahmadov et al. (2015)
RACM2	92	244	Lumped molecule	Goliff et al. (2013)	Goliff et. al. (2015)
CBM-IV	19	47	Lumped structure	Gery et al. (1989)	Foster et al. (2014)
CB05	33	86	Lumped structure	Yarwood et al. (2005)	Dunker et al. (2015)

originally described by Sander et al. (2005), and as subsequently modified by Butler et al. (2011) to include MCM chemistry. In this study, the model is run under conditions representative of 34° N at the equinox (broadly representative of the city of Los Angeles, USA).

Maximum O_3 production is achieved in each model run by balancing the chemical source of radicals and NO_x at each time step by emitting the appropriate amount of NO. These NO_x conditions induce NO_x–VOC-sensitive chemistry. Ambient NO_x conditions are not required as this study calculates the maximum potential of VOCs to produce O_3. Future work should verify the extent to which the maximum potential of VOCs to produce O_3 is reached under ambient NO_x conditions.

VOCs typical of Los Angeles and their initial mixing ratios are taken from Baker et al. (2008), listed in Table 2. Following Butler et al. (2011), the associated emissions required to keep the initial mixing ratios of each VOC constant until noon of the first day were determined for the MCM v3.2. These emissions are subsequently used for each mechanism, ensuring the amount of each VOC emitted was the same in every model run. Methane (CH_4) was fixed at 1.8 ppmv while CO and O_3 were initialised at 200 and 40 ppbv and then allowed to evolve freely.

The VOCs used in this study are assigned to mechanism species following the recommendations from the literature of each mechanism (Table 1), the representation of each VOC in the mechanisms is found in Table 2. Emissions of lumped species are weighted by the carbon number of the mechanism species ensuring the total amount of emitted reactive carbon was the same in each model run.

The MECCA box model is based upon the Kinetic PreProcessor (KPP) (Damian et al., 2002). Hence, all chemical mechanisms were adapted into modularised KPP format. The inorganic gas-phase chemistry described in the MCM v3.2 was used in each run to remove any differences between treatments of inorganic chemistry in each mechanism. Thus, differences between the O_3 produced by the mechanisms are due to the treatment of organic degradation chemistry.

The MCM v3.2 approach to photolysis, dry deposition of VOC oxidation intermediates and RO_2-RO_2 reactions was used for each mechanism; details of these adaptations can be found in the Supplement. Some mechanisms include reactions which are only important in the stratosphere or free troposphere. For example, PAN photolysis is only important in the free troposphere (Harwood et al., 2003) and was removed from MOZART-4, RACM2 and CB05 for the purpose of the study, as this study considers processes occurring within the planetary boundary layer.

2.3 Tagged ozone production potential (TOPP)

This section summarises the tagging approach described in Butler et al. (2011) which is applied in this study.

2.3.1 O_x family and tagging approach

O_3 production and loss is dominated by rapid photochemical cycles, such as Reactions (R1)–(R3). The effects of rapid production and loss cycles can be removed by using chemical families that include rapidly inter-converting species. In this study, we define the O_x family to include O_3, $O(^3P)$, $O(^1D)$, NO_2 and other species involved in fast cycling with NO_2, such as HO_2NO_2 and PAN species. Thus, production of O_x can be used as a proxy for production of O_3.

The tagging approach follows the degradation of emitted VOCs through all possible pathways by labelling every organic degradation product with the name of the emitted VOCs. Thus, each emitted VOC effectively has its own set of degradation reactions. Butler et al. (2011) showed that O_x production can be attributed to the VOCs by following the tags of each VOC.

Table 2. Non-methane volatile organic compounds (NMVOCs) present in Los Angeles. Mixing ratios are taken from Baker et al. (2008) and their representation in each chemical mechanism. The representation of the VOCs in each mechanism is based upon the recommendations of the literature for each mechanism (Table 1).

NMVOCs	Mixing ratio (pptv)	MCM v3.1, v3.2, CRI v2	MOZART-4	RADM2	RACM	RACM2	CBM-IV	CB05
				Alkanes				
Ethane	6610	C2H6	C2H6	ETH	ETH	ETH	0.4 PAR	ETHA
Propane	6050	C3H8	C3H8	HC3	HC3	HC3	1.5 PAR	1.5 PAR
Butane	2340	NC4H10	BIGALK	HC3	HC3	HC3	4 PAR	4 PAR
2-Methylpropane	1240	IC4H10	BIGALK	HC3	HC3	HC3	4 PAR	4 PAR
Pentane	1200	NC5H12	BIGALK	HC5	HC5	HC5	5 PAR	5 PAR
2-Methylbutane	2790	IC5H12	BIGALK	HC5	HC5	HC5	5 PAR	5 PAR
Hexane	390	NC6H14	BIGALK	HC5	HC5	HC5	6 PAR	6 PAR
Heptane	160	NC7H16	BIGALK	HC5	HC5	HC5	7 PAR	7 PAR
Octane	80	NC8H18	BIGALK	HC8	HC8	HC8	8 PAR	8 PAR
				Alkenes				
Ethene	2430	C2H4	C2H4	OL2	ETE	ETE	ETH	ETH
Propene	490	C3H6	C3H6	OLT	OLT	OLT	OLE + PAR	OLE + PAR
Butene	65	BUT1ENE	BIGENE	OLT	OLT	OLT	OLE + 2 PAR	OLE + 2 PAR
2-Methylpropene	130	MEPROPENE	BIGENE	OLI	OLI	OLI	PAR + FORM + ALD2	FORM + 3 PAR
Isoprene	270	C5H8	ISOP	ISO	ISO	ISO	ISOP	ISOP
				Aromatics				
Benzene	480	BENZENE	TOLUENE	TOL	TOL	BEN	PAR	PAR
Toluene	1380	TOLUENE	TOLUENE	TOL	TOL	TOL	TOL	TOL
m-Xylene	410	MXYL	TOLUENE	XYL	XYL	XYM	XYL	XYL
p-Xylene	210	PXYL	TOLUENE	XYL	XYL	XYP	XYL	XYL
o-Xylene	200	OXYL	TOLUENE	XYL	XYL	XYO	XYL	XYL
Ethylbenzene	210	EBENZ	TOLUENE	TOL	TOL	TOL	TOL + PAR	TOL + PAR

O_x production from lumped-mechanism species are reassigned to the VOCs of Table 2 by scaling the O_x production of the mechanism species by the fractional contribution of each represented VOC. For example, TOL in RACM2 represents toluene and ethylbenzene with fractional contributions of 0.87 and 0.13 to TOL emissions. Scaling the O_x production from TOL by these factors gives the O_x production from toluene and ethylbenzene in RACM2.

Many reduced mechanisms use an operator species as a surrogate for RO_2 during VOC degradation enabling these mechanisms to produce O_x while minimising the number of RO_2 species represented. O_x production from operator species is assigned as O_x production from the organic degradation species producing the operator. This allocation technique is also used to assign O_x production from HO_2 via Reaction (R7).

2.3.2 Definition of TOPP

Attributing O_x production to individual VOCs using the tagging approach is the basis for calculating the TOPP of a VOC, which is defined as the number of O_x molecules produced per emitted molecule of VOC. The TOPP value of a VOC that is not represented explicitly in a chemical mechanism is calculated by multiplying the TOPP value of the mechanism species representing the VOCs by the ratio of the carbon numbers of the VOCs to the mechanism species. For example, CB05 represents hexane as 6 PAR, so the TOPP value of hexane in the CB05 is 6 times the TOPP of PAR. MOZART-4 represents hexane with the five carbon species BIGALK. Thus, hexane emissions are represented molecule for molecule as $\frac{6}{5}$ of the equivalent number of molecules of BIGALK, and the TOPP value of hexane in MOZART-4 is calculated by multiplying the TOPP value of BIGALK by $\frac{6}{5}$.

3 Results

3.1 Ozone time series and O_x production budgets

Figure 1 shows the time series of O_3 mixing ratios obtained with each mechanism. There is an 8 ppbv difference in O_3 mixing ratios on the first day between RADM2, which has the highest O_3, and RACM2, which has the lowest O_3 mixing ratios when not considering the outlier time series of RACM. The difference between RADM2 and RACM, the low outlier, was 21 ppbv on the first day. The O_3 mixing ratios in

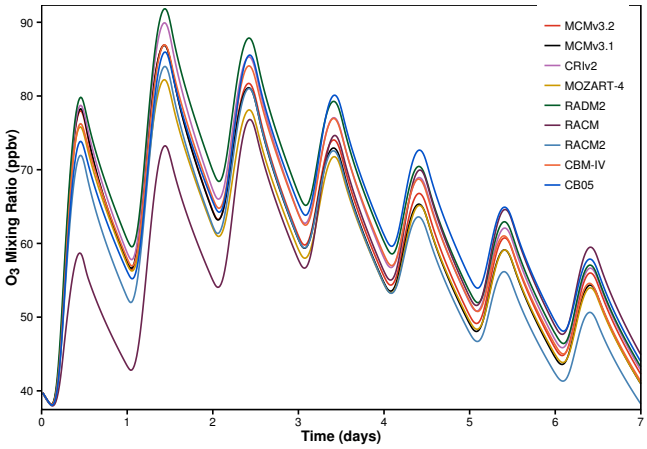

Figure 1. Time series of O_3 mixing ratios obtained using each mechanism.

the CRI v2 are larger than those in the MCM v3.1, which is similar to the results in Jenkin et al. (2008) where the O_3 mixing ratios of the CRI v2 and MCM v3.1 are compared over a 5-day period.

The O_3 mixing ratios in Fig. 1 are influenced by the approaches used in developing the chemical mechanisms and not a function of the explicitness of the chemical mechanism. For example, the O_3 mixing ratios obtained using the Carbon Bond mechanisms (CBM-IV and CB05) compare well with the MCM despite both Carbon Bond mechanisms having ~ 1 % of the number of reactions in the MCM v3.2. Also, the O_3 mixing ratios from RACM2 and RADM2 show similar absolute differences from that of the MCM despite RACM2 having more than double the number of reactions of RADM2.

The day-time O_x production budgets allocated to individual VOCs for each mechanism are shown in Fig. 2. The relationships between O_3 mixing ratios in Fig. 1 are mirrored in Fig. 2 where mechanisms producing high amounts of O_x also have high O_3 mixing ratios. The conditions in the box model lead to a daily maximum of OH that increases with each day leading to an increase on each day in both the reaction rate of the OH oxidation of CH_4 and the daily contribution of CH_4 to O_x production.

The first-day mixing ratios of O_3 in RACM are lower than other mechanisms due to a lack of O_x production from aromatic VOCs on the first day in RACM (Fig. 2). Aromatic degradation chemistry in RACM results in net loss of O_x on the first day, described later in Sect. 3.2.1.

RADM2 is the only reduced mechanism that produces higher O_3 mixing ratios than the more detailed mechanisms (MCM v3.2, MCM v3.1 and CRI v2). Higher mixing ratios of O_3 in RADM2 are produced due to increased O_x production from propane compared to the MCM v3.2; on the first day, the O_x production from propane in RADM2 is triple that of the MCM v3.2 (Fig. 2). Propane is represented as HC3 in

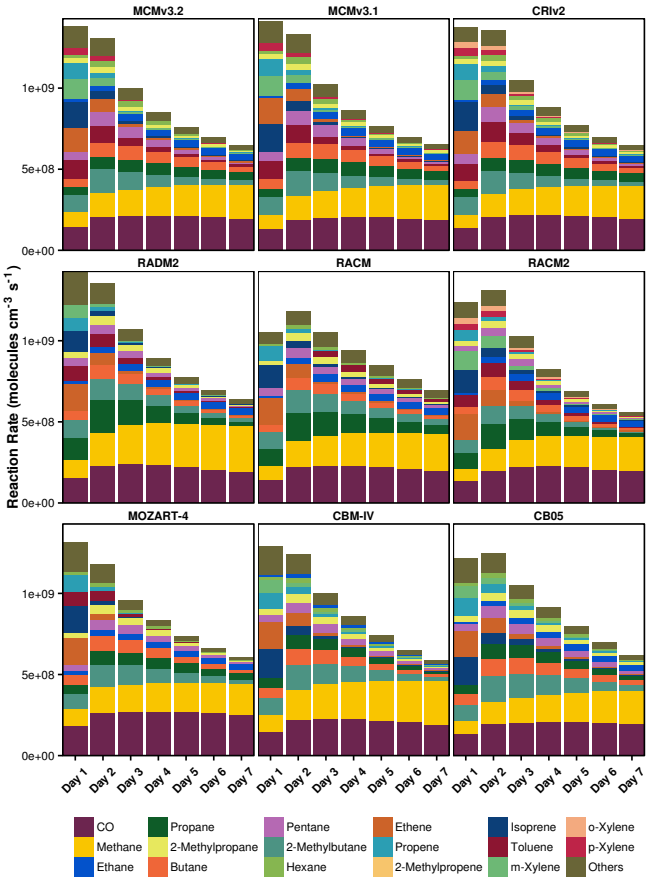

Figure 2. Day-time O_x production budgets in each mechanism allocated to individual VOCs.

RADM2 (Stockwell et al., 1990) and the degradation of HC3 has a lower yield of the less-reactive ketones compared to the MCM. The further degradation of ketones hinders O_x production due to the low OH reactivity and photolysis rate of ketones. Secondary degradation of HC3 proceeds through the degradation of acetaldehyde (CH_3CHO) propagating O_x production through the reactions of CH_3CO_3 and CH_3O_2 with NO. Thus, the lower ketone yields lead to increased O_x production from propane degradation in RADM2 compared to the MCM v3.2.

3.2 Time-dependent O_x production

Time series of daily TOPP values for each VOC are presented in Fig. 3 and the cumulative TOPP values at the end of the model run obtained for each VOC using each of the mechanisms, normalised by the number of atoms of C in each VOC are presented in Table 3. In the MCM and CRI v2, the cumulative TOPP values obtained for each VOC show that by the end of the model run, larger alkanes have produced more O_x per unit of reactive C than alkenes or aromatic VOCs. By the end of the runs using the lumped-structure mechanisms (CBM-IV and CB05), alkanes produce similar

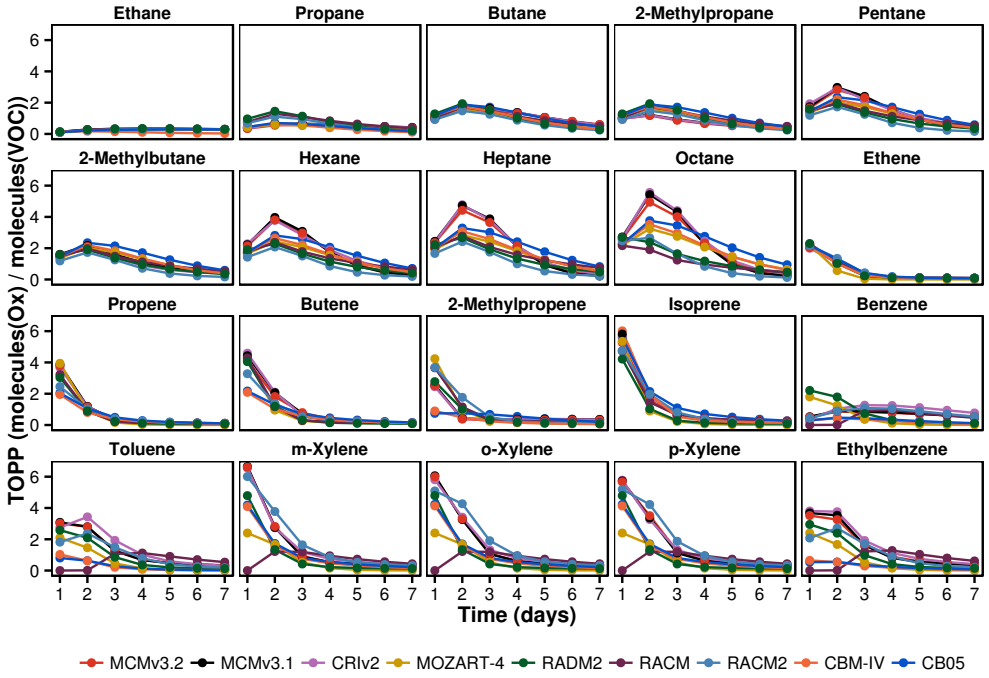

Figure 3. TOPP value time series using each mechanism for each VOC.

Table 3. Cumulative TOPP values at the end of the model run for all VOCs with each mechanism, normalised by the number of C atoms in each VOC.

NMVOCs	MCM v3.2	MCM v3.1	CRI v2	MOZART-4	RADM2	RACM	RACM2	CBM-IV	CB05
				Alkanes					
Ethane	0.9	1.0	0.9	0.9	1.0	1.0	0.9	0.3	0.9
Propane	1.1	1.2	1.2	1.1	1.8	1.8	1.4	0.9	1.0
Butane	2.0	2.0	2.0	1.7	1.8	1.8	1.4	1.7	2.1
2-Methylpropane	1.3	1.3	1.3	1.7	1.8	1.8	1.4	1.7	2.1
Pentane	2.1	2.1	2.2	1.7	1.5	1.6	1.1	1.7	2.1
2-Methylbutane	1.6	1.6	1.5	1.7	1.5	1.6	1.1	1.7	2.1
Hexane	2.1	2.1	2.2	1.7	1.5	1.6	1.1	1.7	2.1
Heptane	2.0	2.1	2.2	1.7	1.5	1.6	1.1	1.7	2.1
Octane	2.0	2.0	2.2	1.7	1.2	1.0	1.0	1.7	2.1
				Alkenes					
Ethene	1.9	1.9	1.9	1.4	2.0	2.0	2.2	1.9	2.2
Propene	1.9	2.0	1.9	1.7	1.5	1.6	1.5	1.2	1.4
Butene	1.9	2.0	2.0	1.5	1.5	1.6	1.5	0.8	0.9
2-Methylpropene	1.1	1.2	1.2	1.5	1.1	1.5	1.6	0.5	0.5
Isoprene	1.8	1.8	1.8	1.3	1.2	1.6	1.7	1.9	2.1
				Aromatics					
Benzene	0.8	0.8	1.1	0.6	0.9	0.6	0.9	0.3	0.3
Toluene	1.3	1.3	1.5	0.6	0.9	0.6	1.0	0.3	0.3
m-Xylene	1.5	1.5	1.6	0.6	0.9	0.6	1.7	0.9	1.0
p-Xylene	1.5	1.5	1.6	0.6	0.9	0.6	1.7	0.9	1.0
o-Xylene	1.5	1.5	1.6	0.6	0.9	0.6	1.7	0.9	1.0
Ethylbenzene	1.3	1.4	1.5	0.6	0.9	0.6	1.0	0.2	0.3

amounts of O_x per reactive C, while aromatic VOCs and some alkenes produce less O_x per reactive C than the MCM. However, in lumped-molecule mechanisms (MOZART-4, RADM2, RACM, RACM2), practically all VOCs produce less O_x per reactive C than the MCM by the end of the run. This lower efficiency of O_x production from many individual VOCs in lumped-molecule and lumped-structure mechanisms would lead to an underestimation of O_3 levels downwind of an emission source, and a smaller contribution to background O_3 when using lumped-molecule and lumped-structure mechanisms.

The lumped-intermediate mechanism (CRI v2) produces the most similar O_x to the MCM v3.2 for each VOC, seen in Fig. 3 and Table 3. Higher variability in the time-dependent O_x production is evident for VOCs represented by lumped-mechanism species. For example, 2-methylpropene, represented in the reduced mechanisms by a variety of lumped species, has a higher spread in time-dependent O_x production than ethene, which is explicitly represented in each mechanism.

In general, the largest differences in O_x produced by aromatic and alkene species are on the first day of the simulations, while the largest inter-mechanism differences in O_x produced by alkanes are on the second and third days of the simulations. The reasons for these differences in behaviour will be explored in Sect. 3.2.1, which examines differences in first day O_x production between the chemical mechanisms, and Sect. 3.2.2, which examines the differences in O_x production on subsequent days.

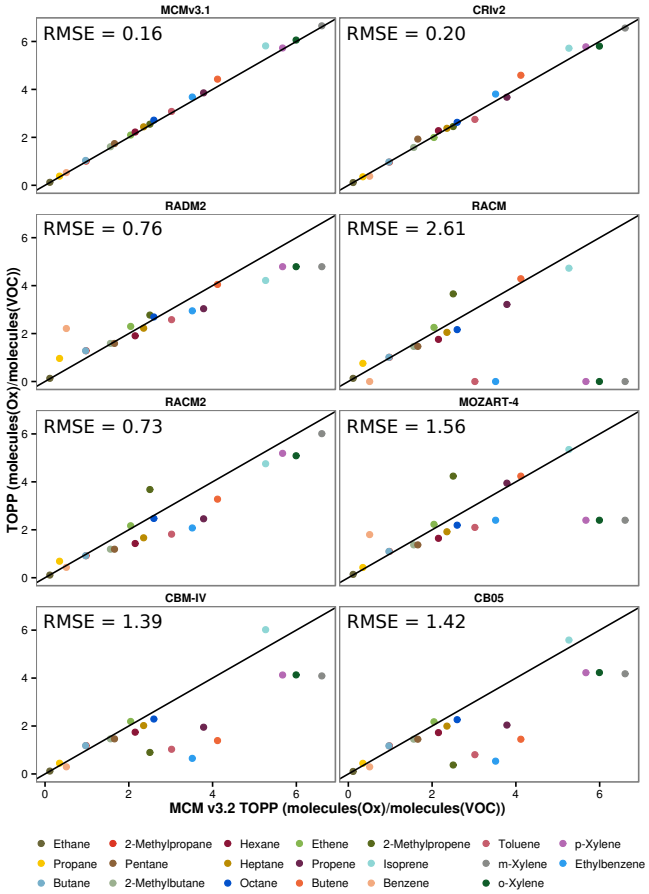

Figure 4. The first-day TOPP values for each VOC calculated using MCM v3.2 and the corresponding values in each mechanism. The root mean square error (RMSE) of each set of TOPP values is also displayed. The black line is the 1 : 1 line.

3.2.1 First-day ozone production

The first-day TOPP values of each VOC from each mechanism, representing O_3 production from freshly emitted VOCs near their source region, are compared to those obtained with the MCM v3.2 in Fig. 4. The root mean square error (RMSE) of all first-day TOPP values in each mechanism relative to those in the MCM v3.2 are also included in Fig. 4. The RMSE value of the CRI v2 shows that first-day O_x production from practically all the individual VOC matches that in the MCM v3.2. All other reduced mechanisms have much larger RMSE values indicating that the first-day O_x production from the majority of the VOCs differs from that in the MCM v3.2.

The reduced complexity of reduced mechanisms means that aromatic VOCs are typically represented by one or two mechanism species leading to differences in O_x production of the actual VOCs compared to the MCM v3.2. For example, all aromatic VOCs in MOZART-4 are represented as toluene, thus less-reactive aromatic VOCs, such as benzene, produce higher O_x whilst more-reactive aromatic VOCs, such as the xylenes, produce less O_x in MOZART-4 than the MCM v3.2. RACM2 includes explicit species representing benzene, toluene and each xylene resulting in O_x production that is the most similar to the MCM v3.2 than other reduced mechanisms.

Figure 3 shows a high spread in O_x production from aromatic VOCs on the first day indicating that aromatic degradation is treated differently between mechanisms. Toluene degradation is examined in more detail by comparing the reactions contributing to O_x production and loss in each mechanism, shown in Fig. 5. These reactions are determined by following the "toluene" tags in the tagged version of each mechanism.

Toluene degradation in RACM includes several reactions consuming O_x that are not present in the MCM, resulting in net loss of O_x on the first 2 days. Ozonolysis of the cresol OH adduct mechanism species, ADDC, contributes significantly to O_x loss in RACM. This reaction was included in RACM due to improved cresol product yields when comparing RACM predictions with experimental data (Stockwell et al., 1997). Other mechanisms that include cresol OH adduct species do not include ozonolysis and these reactions are not included in the updated RACM2.

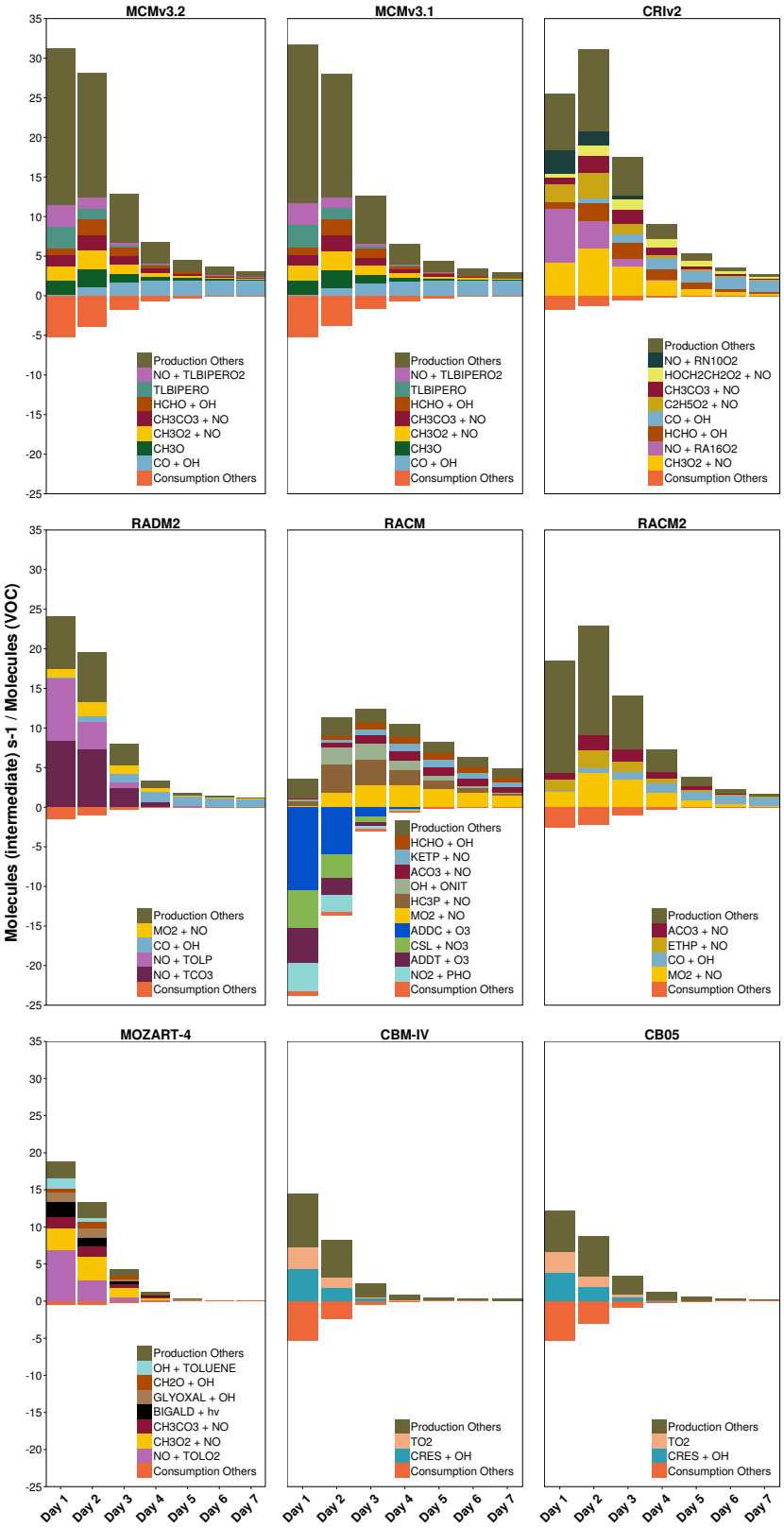

Figure 5. Day-time O_x production and loss budgets allocated to the responsible reactions during toluene degradation in all mechanisms. These reactions are presented using the species defined in each mechanism in Table 1.

The total O_x produced on the first day during toluene degradation in each reduced mechanism is less than that in the MCM v3.2 (Fig. 5). Less O_x is produced in all reduced mechanisms due to a faster breakdown of the VOCs into smaller fragments than the MCM, described later in Sect. 3.3. Moreover, in CBM-IV and CB05, less O_x is produced during toluene degradation as reactions of the toluene degradation products CH_3O_2 and CO do not contribute to the O_x production budgets, which is not the case in any other mechanism (Fig. 5).

Maximum O_x production from toluene degradation in CRI v2 and RACM2 is reached on the second day in contrast to the MCM v3.2 which produces peak O_x on the first day. The second-day maximum of O_x production in CRI v2 and RACM2 from toluene degradation results from more efficient production of unsaturated dicarbonyls than the MCM v3.2. The degradation of unsaturated dicarbonyls produces peroxy radicals such as $C_2H_5O_2$ which promote O_x production via reactions with NO.

Unsaturated aliphatic VOCs generally produce similar amounts of O_x between mechanisms, especially explicitly represented VOCs, such as ethene and isoprene. On the other hand, unsaturated aliphatic VOCs that are not explicitly represented produce differing amounts of O_x between mechanisms (Fig. 3). For example, the O_x produced during 2-methylpropene degradation varies between mechanisms; differing rate constants of initial oxidation reactions and non-realistic secondary chemistry lead to these differences; further details are found in the Supplement.

Non-explicit representations of aromatic and unsaturated aliphatic VOCs coupled with differing degradation chemistry and a faster breakdown into smaller-size degradation products results in different O_x production in lumped-molecule and lumped-structure mechanisms compared to the MCM v3.2.

3.2.2 Ozone production on subsequent days

Alkane degradation in CRI v2 and both MCMs produces a second-day maximum in O_x that increases with alkane carbon number (Fig. 3). The increase in O_x production on the second day is reproduced for each alkane by the reduced mechanisms, except octane in RADM2, RACM and RACM2. However, larger alkanes produce less O_x than the MCM on the second day in all lumped-molecule and lumped-structure mechanisms.

The lumped-molecule mechanisms (MOZART-4, RADM2, RACM and RACM2) represent many alkanes by mechanism species which may lead to unrepresentative secondary chemistry for alkane degradation. For example, 3 times more O_x is produced during the degradation of propane in RADM2 than the MCM v3.2 on the first day (Fig. 2). Propane is represented in RADM2 by the mechanism species HC3 which also represents other classes of VOCs, such as alcohols. The secondary chemistry of HC3 is tailored to produce O_x from these different VOCs and differs from alkane degradation in the MCM v3.2 by producing less ketones in RADM2.

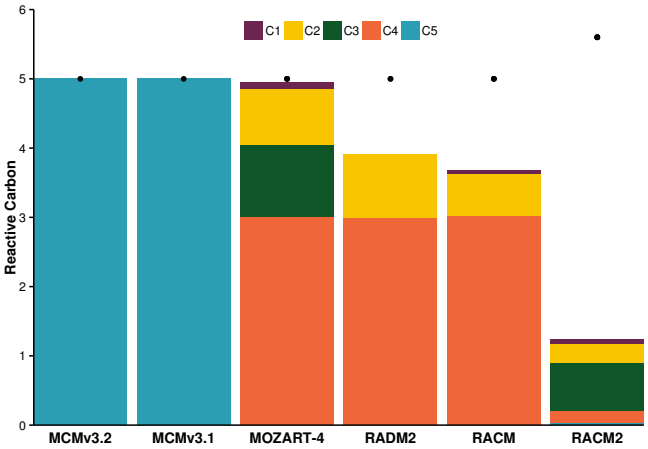

Figure 6. The distribution of reactive carbon in the products of the reaction between NO and the pentyl peroxy radical in lumped-molecule mechanisms compared to the MCM. The black dot represents the reactive carbon of the pentyl peroxy radical.

As will be shown in Sect. 3.3, another feature of reduced mechanisms is that the breakdown of emitted VOCs into smaller-sized degradation products is faster than the MCM. Alkanes are broken down quicker in CBM-IV, CB05, RADM2, RACM and RACM2 through a higher rate of reactive carbon loss than the MCM v3.2 (shown for pentane and octane in Fig. 8); reactive carbon is lost through reactions not conserving carbon. Despite many degradation reactions of alkanes in MOZART-4 almost conserving carbon, the organic products have less reactive carbon than the organic reactant also speeding up the breakdown of the alkane compared to the MCM v3.2.

For example, Fig. 6 shows the distribution of reactive carbon in the reactants and products from the reaction of NO with the pentyl peroxy radical in both MCMs and each lumped-molecule mechanism. In all the lumped-molecule mechanisms, the individual organic products have less reactive carbon than the organic reactant. Moreover, in RADM2, RACM and RACM2, this reaction does not conserve reactive carbon leading to faster loss rates of reactive carbon.

The faster breakdown of alkanes in lumped-molecule and lumped-structure mechanisms on the first day limits the amount of O_x produced on the second day, as less of the larger-sized degradation products are available for further degradation and O_x production.

3.3 Treatment of degradation products

The time-dependent O_x production of the different VOCs in Fig. 3 results from the varying rates at which VOCs break up into smaller fragments (Butler et al., 2011). Varying breakdown rates of the same VOCs between mechanisms could

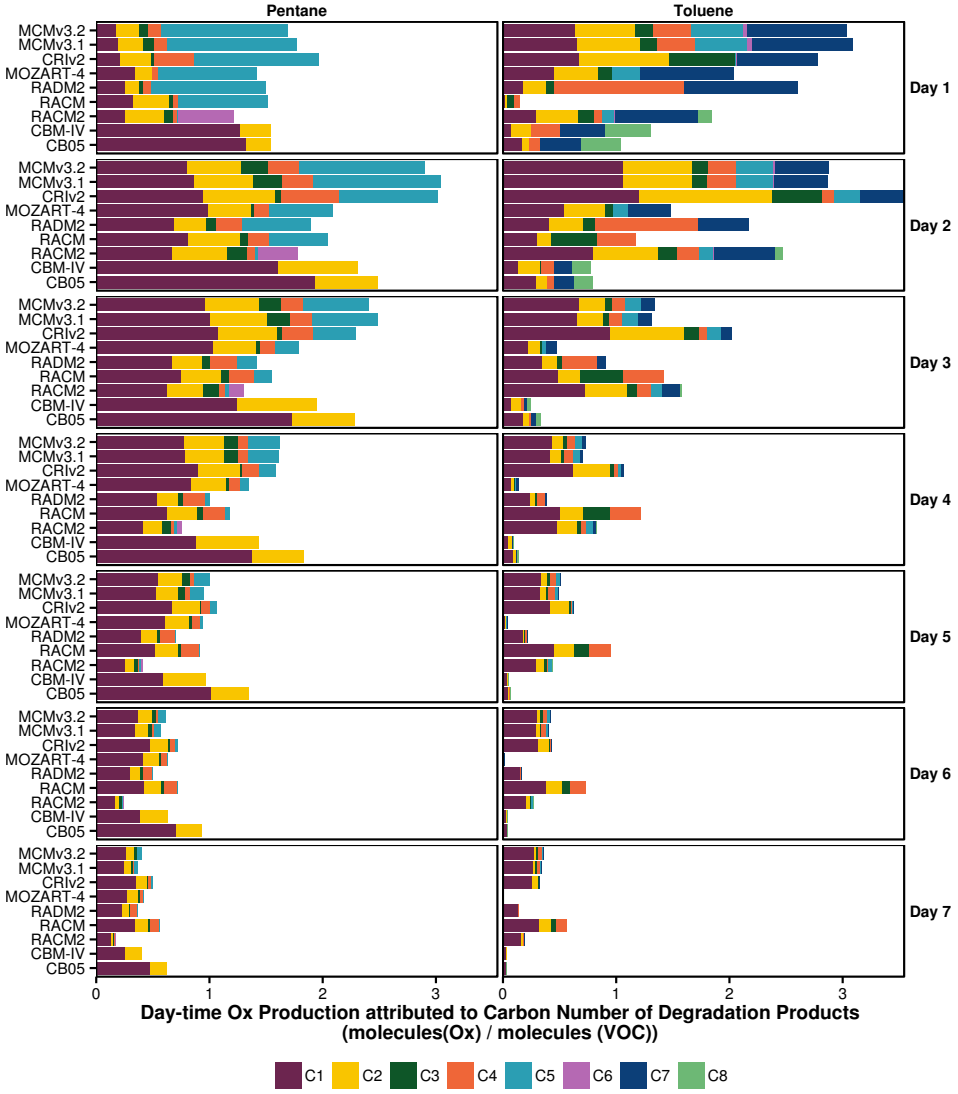

Figure 7. Day-time O_x production during pentane and toluene degradation is attributed to the number of carbon atoms of the degradation products for each mechanism.

explain the different time-dependent O_x production between mechanisms. The breakdown of pentane and toluene between mechanisms is compared in Fig. 7 by allocating the O_x production to the number of carbon atoms in the degradation products responsible for O_x production on each day of the model run in each mechanism. Some mechanism species in RADM2, RACM and RACM2 have fractional carbon numbers (Stockwell et al., 1990, 1997; Goliff et al., 2013) and O_x production from these species was reassigned as O_x production of the nearest integral carbon number.

The degradation of pentane, a five-carbon VOC, on the first day in the MCM v3.2 produces up to 50 % more O_x from degradation products also having five carbon atoms than any reduced mechanism. Moreover, the contribution of the degradation products having five carbon atoms in the MCM v3.2 is consistently higher throughout the model run than in reduced mechanisms (Fig. 7). Despite producing less total O_x, reduced mechanisms produce up to double the amount of O_x from degradation products with one carbon atom than in the MCM v3.2. The lower contribution of larger degradation products indicates that pentane is generally broken down faster in reduced mechanisms, consistent with the specific example shown for the breakdown of the pentyl peroxy radical in Fig. 6.

The rate of change in reactive carbon during pentane, octane and toluene degradation was determined by multiplying the rate of each reaction occurring during pentane, octane and toluene degradation by its net change in carbon, shown in Fig. 8. Pentane is broken down faster in CBM-IV, CB05, RADM2, RACM and RACM2 by losing reactive carbon more quickly than the MCM v3.2. MOZART-4 also breaks pentane down into smaller-sized products quicker

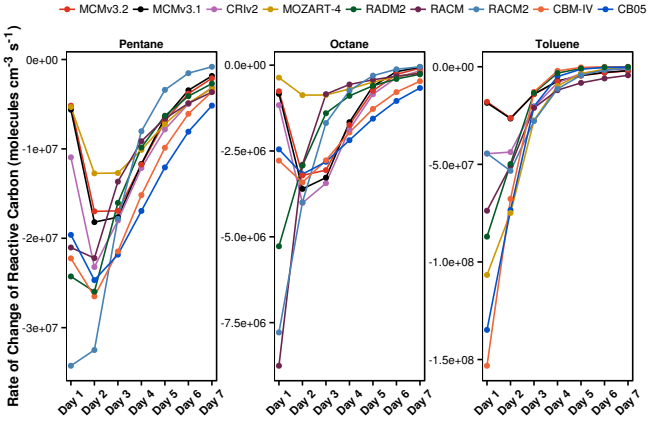

Figure 8. Daily rate of change in reactive carbon during pentane, octane and toluene degradation. Octane is represented by the five carbon species, BIGALK, in MOZART-4.

than the MCM v3.2 as reactions during pentane degradation in MOZART-4 have organic products whose carbon number is less than the organic reactant, described in Sect. 3.2.2. The faster breakdown of pentane on the first day limits the amount of reactive carbon available to produce further O_x on subsequent days leading to lower O_x production after the first day in reduced mechanisms.

Figure 3 showed that octane degradation produces peak O_x on the first day in RADM2, RACM and RACM2 in contrast to all other mechanisms where peak O_x is produced on the second day. Octane degradation in RADM2, RACM and RACM2 loses reactive carbon much faster than any other mechanism on the first day so that there are not enough degradation products available to produce peak O_x on the second day (Fig. 8). This loss of reactive carbon during alkane degradation leads to the lower accumulated ozone production from these VOCs shown in Table 3.

As seen in Fig. 3, O_x produced during toluene degradation has a high spread between the mechanisms. Figure 7 shows differing distributions of the sizes of the degradation products that produce O_x. All reduced mechanisms omit O_x production from at least one degradation fragment size which produces O_x in the MCM v3.2, indicating that toluene is also broken down more quickly in the reduced mechanisms than the more explicit mechanisms. For example, toluene degradation in RACM2 does not produce O_x from degradation products with six carbons, as is the case in the MCM v3.2. Figure 8 shows that all reduced mechanisms lose reactive carbon during toluene degradation faster than the MCM v3.2. Thus, the degradation of aromatic VOCs in reduced mechanisms are unable to produce similar amounts of O_x as the explicit mechanisms.

4 Conclusions

Tagged ozone production potentials (TOPPs) were used to compare O_x production during VOC degradation in reduced chemical mechanisms to the near-explicit MCM v3.2. First-day mixing ratios of O_3 are similar to the MCM v3.2 for most mechanisms; the O_3 mixing ratios in RACM were much lower than the MCM v3.2 due to a lack of O_x production from the degradation of aromatic VOCs. Thus, RACM may not be the appropriate chemical mechanism when simulating atmospheric conditions having a large fraction of aromatic VOCs.

The lumped-intermediate mechanism, CRI v2, produces the most similar amounts of O_x to the MCM v3.2 for each VOC. The largest differences between O_x production in CRI v2 and MCM v3.2 were obtained for aromatic VOCs; however, overall these differences were much lower than any other reduced mechanism. Thus, when developing chemical mechanisms, the technique of using lumped-intermediate species whose degradation are based upon more detailed mechanism should be considered.

Many VOCs are broken down into smaller-sized degradation products faster on the first day in reduced mechanisms than the MCM v3.2 leading to lower amounts of larger-sized degradation products that can further degrade and produce O_x. Thus, many VOCs in reduced mechanisms produce a lower maximum of O_x and lower total O_x per reactive C by the end of the run than the MCM v3.2. This lower O_x production from many VOCs in reduced mechanisms leads to lower O_3 mixing ratios compared to the MCM v3.2.

Alkanes produce maximum O_3 on the second day of simulations and this maximum is lower in reduced mechanisms than the MCM v3.2 due to the faster breakdown of alkanes into smaller-sized degradation products on the first day. The lower maximum in O_3 production during alkane degradation in reduced mechanisms leads to an underestimation of the O_3 levels downwind of VOC emissions and an underestimation of the VOC contribution to tropospheric background O_3 when using reduced mechanisms in regional or global modelling studies.

This study has determined the maximum potential of VOCs represented in reduced mechanisms to produce O_3; this potential may not be reached as ambient NO_x conditions may not induce NO_x–VOC-sensitive chemistry. Moreover, the maximum potential of VOCs to produce O_3 may not be reached when using these reduced mechanisms in 3-D models due to the influence of additional processes, such as mixing and meteorology. Future work shall examine the extent to which the maximum potential of VOCs to produce O_3 in reduced chemical mechanisms is reached using ambient NO_x conditions and including processes found in 3-D models.

The Supplement related to this article is available online at doi:10.5194/acp-15-8795-2015-supplement.

Acknowledgements. The authors would like to thank Mike Jenkin and William Stockwell for their helpful reviews, as well as Mark Lawrence and Peter J. H. Builtjes for valuable discussions during the preparation of this manuscript.

Edited by: R. Harley

References

Ahmadov, R., McKeen, S., Trainer, M., Banta, R., Brewer, A., Brown, S., Edwards, P. M., de Gouw, J. A., Frost, G. J., Gilman, J., Helmig, D., Johnson, B., Karion, A., Koss, A., Langford, A., Lerner, B., Olson, J., Oltmans, S., Peischl, J., Pétron, G., Pichugina, Y., Roberts, J. M., Ryerson, T., Schnell, R., Senff, C., Sweeney, C., Thompson, C., Veres, P. R., Warneke, C., Wild, R., Williams, E. J., Yuan, B., and Zamora, R.: Understanding high wintertime ozone pollution events in an oil- and natural gas-producing region of the western US, Atmos. Chem. Phys., 15, 411–429, doi:10.5194/acp-15-411-2015, 2015.

Atkinson, R.: Atmospheric chemistry of VOCs and NO_x, Atmos. Environ., 34, 2063–2101, 2000.

Baker, A. K., Beyersdorf, A. J., Doezema, L. A., Katzenstein, A., Meinardi, S., Simpson, I. J., Blake, D. R., and Rowland, F. S.: Measurements of nonmethane hydrocarbons in 28 United States cities, Atmos. Environ., 42, 170–182, 2008.

Baklanov, A., Schlünzen, K., Suppan, P., Baldasano, J., Brunner, D., Aksoyoglu, S., Carmichael, G., Douros, J., Flemming, J., Forkel, R., Galmarini, S., Gauss, M., Grell, G., Hirtl, M., Joffre, S., Jorba, O., Kaas, E., Kaasik, M., Kallos, G., Kong, X., Korsholm, U., Kurganskiy, A., Kushta, J., Lohmann, U., Mahura, A., Manders-Groot, A., Maurizi, A., Moussiopoulos, N., Rao, S. T., Savage, N., Seigneur, C., Sokhi, R. S., Solazzo, E., Solomos, S., Sørensen, B., Tsegas, G., Vignati, E., Vogel, B., and Zhang, Y.: Online coupled regional meteorology chemistry models in Europe: current status and prospects, Atmos. Chem. Phys., 14, 317–398, doi:10.5194/acp-14-317-2014, 2014.

Bloss, C., Wagner, V., Jenkin, M. E., Volkamer, R., Bloss, W. J., Lee, J. D., Heard, D. E., Wirtz, K., Martin-Reviejo, M., Rea, G., Wenger, J. C., and Pilling, M. J.: Development of a detailed chemical mechanism (MCMv3.1) for the atmospheric oxidation of aromatic hydrocarbons, Atmos. Chem. Phys., 5, 641–664, doi:10.5194/acp-5-641-2005, 2005.

Butler, T. M., Lawrence, M. G., Taraborrelli, D., and Lelieveld, J.: Multi-day ozone production potential of volatile organic compounds calculated with a tagging approach, Atmos. Environ., 45, 4082–4090, 2011.

Carter, W. P. L.: Development of ozone reactivity scales for volatile organic compounds, J. Air Waste Manage., 44, 881–899, 1994.

Damian, V., Sandu, A., Damian, M., Potra, F., and Carmichael, G.: The kinetic preprocessor KPP – a software environment for solving chemical kinetics, Comput. Chem. Eng., 26, 1567–1579, 2002.

Derwent, R. G., Jenkin, M. E., and Saunders, S. M.: Photochemical ozone creation potentials for a large number of reactive hydrocarbons under European conditions, Atmos. Environ., 30, 181–199, 1996.

Derwent, R. G., Jenkin, M. E., Saunders, S. M., and Pilling, M. J.: Photochemical ozone creation potentials for organic compounds in Northwest Europe calculated with a master chemical mechanism, Atmos. Environ., 32, 2429–2441, 1998.

Derwent, R. G., Jenkin, M. E., Pilling, M. J., Carter, W. P. L., and Kaduwela, A.: Reactivity scales as comparative tools for chemical mechanisms, J. Air Waste Manage., 60, 914–924, 2010.

Derwent, R. G., Utember, S. R., Jenkin, M. E., and Shallcross, D. E.: Tropospheric ozone production regions and the intercontinental origins of surface ozone over Europe, Atmos. Environ., 112, 216–224, 2015

Dodge, M.: Chemical oxidant mechanisms for air quality modeling: critical review, Atmos. Environ., 34, 2103–2130, 2000.

Dunker, A. M., Kumar, S., and Berzins, P. H.: A comparison of chemical mechanisms used in atmospheric models, Atmos. Environ., 18, 311–321, 1984.

Dunker, A. M., Koo, B,, and Yarwood, G.: Source Apportionment of the Anthropogenic Increment to Ozone, Formaldehyde, and Nitrogen Dioxide by the Path- Integral Method in a 3D Model, Environ. Sci. Technol., 49, 6751–6759, 2015.

EEA: Air quality in Europe – 2014 report, Tech. Rep. 5/2014, European Environmental Agency, Publications Office of the European Union, doi:10.2800/22847, 2014.

Emmerson, K. M. and Evans, M. J.: Comparison of tropospheric gas-phase chemistry schemes for use within global models, Atmos. Chem. Phys., 9, 1831–1845, doi:10.5194/acp-9-1831-2009, 2009.

Emmons, L. K., Walters, S., Hess, P. G., Lamarque, J.-F., Pfister, G. G., Fillmore, D., Granier, C., Guenther, A., Kinnison, D., Laepple, T., Orlando, J., Tie, X., Tyndall, G., Wiedinmyer, C., Baughcum, S. L., and Kloster, S.: Description and evaluation of the Model for Ozone and Related chemical Tracers, version 4 (MOZART-4), Geosci. Model Dev., 3, 43–67, doi:10.5194/gmd-3-43-2010, 2010.

Foster, P. N., Prentice, I. C., Morfopoulos, C., Siddall, M., and van Weele, M.: Isoprene emissions track the seasonal cycle of canopy temperature, not primary production: evidence from remote sensing, Biogeosciences, 11, 3437–3451, doi:10.5194/bg-11-3437-2014, 2014.

Gery, M. W., Whitten, G. Z., Killus, J. P., and Dodge, M. C.: A photochemical kinetics mechanism for urban and regional scale computer modeling, J. Geophys. Res., 94, 12925–12956, 1989.

Goliff, W. S., Stockwell, W. R., and Lawson, C. V.: The regional atmospheric chemistry mechanism, version 2, Atmos. Environ., 68, 174–185, 2013.

Goliff, W. S., Luria, M., Blake, D. R., Zielinska, B., Hallar, G., Valente, R. J., Lawson, C. V., and Stockwell, W. R.: Nighttime air quality under desert conditions, Atmos. Environ., 114, 102–111, 2015.

Harwood, M., Roberts, J., Frost, G., Ravishankara, A., and Burkholder, J.: Photochemical studies of $CH_3C(O)OONO_2$ (PAN) and $CH_3CH_2C(O)OONO_2$ (PPN): NO_3 quantum yields, J. Phys. Chem. A, 107, 1148–1154, 2003.

Hogo, H. and Gery, M.: User's guide for executing OZIPM-4 (Ozone Isopleth Plotting with Optional Mechanisms, Version 4) with CBM-IV (Carbon-Bond Mechanisms-IV) or optional mechanisms. Volume 1. Description of the ozone isopleth plotting package. Version 4, Tech. rep., US Environmental Protection Agency, Durham, North Carolina, USA, 1989.

Hou, X., Zhu, B., Fei, D., and Wang, D.: The impacts of summer monsoons on the ozone budget of the atmospheric boundary

layer of the Asia-Pacific region, Sci. Total Environ., 502, 641–649, 2015.

HTAP: Hemispheric Transport of Air Pollution 2010, Part A: Ozone and Particulate Matter, Air Pollution Studies No.17, Geneva, Switzerland, 2010.

Jenkin, M. E. and Clemitshaw, K. C.: Ozone and other secondary photochemical pollutants: chemical processes governing their formation in the planetary boundary layer, Atmos. Environ., 34, 2499–2527, 2000.

Jenkin, M. E., Saunders, S. M., and Pilling, M. J.: The tropospheric degradation of volatile organic compounds: a protocol for mechanism development, Atmos. Environ., 31, 81–104, 1997.

Jenkin, M. E., Saunders, S. M., Wagner, V., and Pilling, M. J.: Protocol for the development of the Master Chemical Mechanism, MCM v3 (Part B): tropospheric degradation of aromatic volatile organic compounds, Atmos. Chem. Phys., 3, 181–193, doi:10.5194/acp-3-181-2003, 2003.

Jenkin, M. E., Watson, L. A., Utembe, S. R., and Shallcross, D. E.: A Common Representative Intermediates (CRI) mechanism for VOC degradation. Part 1: Gas phase mechanism development, Atmos. Environ., 42, 7185–7195, 2008.

Kleinman, L. I.: Seasonal dependence of boundary layer peroxide concentration: the low and high NO_x regimes, J. Geophys. Res., 96, 20721–20733, 1991.

Kleinman, L. I.: Low and high NO_x tropospheric photochemistry, J. Geophys. Res., 99, 16831–16838, 1994.

Koss, A. R., de Gouw, J., Warneke, C., Gilman, J. B., Lerner, B. M., Graus, M., Yuan, B., Edwards, P., Brown, S. S., Wild, R., Roberts, J. M., Bates, T. S., and Quinn, P. K.: Photochemical aging of volatile organic compounds associated with oil and natural gas extraction in the Uintah Basin, UT, during a wintertime ozone formation event, Atmos. Chem. Phys., 15, 5727–5741, doi:10.5194/acp-15-5727-2015, 2015.

Kuhn, M., Builtjes, P. J. H., Poppe, D., Simpson, D., Stockwell, W. R., Andersson-Sköld, Y., Baart, A., Das, M., Fiedler, F., Hov, Ø., Kirchner, F., Makar, P. A., Milford, J. B., Roemer, M. G. M., Ruhnke, R., Strand, A., Vogel, B., and Vogel, H.: Intercomparison of the gas-phase chemistry in several chemistry and transport models, Atmos. Environ., 32, 693–709, 1998.

Li, J., Georgescu, M., Hyde, P., Mahalov, A., and Moustaoui, M.: Achieving accurate simulations of urban impacts on ozone at high resolution, Environ. Res. Lett., 9, 114019, doi:10.1088/1748-9326/9/11/114019, 2014.

Lidster, R. T., Hamilton, J. F., Lee, J. D., Lewis, A. C., Hopkins, J. R., Punjabi, S., Rickard, A. R., and Young, J. C.: The impact of monoaromatic hydrocarbons on OH reactivity in the coastal UK boundary layer and free troposphere, Atmos. Chem. Phys., 14, 6677–6693, doi:10.5194/acp-14-6677-2014, 2014.

Rickard, A., Young, J., Pilling, M., Jenkin. M., Pascoe, S., and Saunders S.: The Master Chemical Mechanism Version MCM v3.2, available at: http://mcm.leeds.ac.uk/MCMv3.2/, last access: 15 July 2015.

Sander, R., Kerkweg, A., Jöckel, P., and Lelieveld, J.: Technical note: The new comprehensive atmospheric chemistry module MECCA, Atmos. Chem. Phys., 5, 445–450, doi:10.5194/acp-5-445-2005, 2005.

Saunders, S. M., Jenkin, M. E., Derwent, R. G., and Pilling, M. J.: Protocol for the development of the Master Chemical Mechanism, MCM v3 (Part A): tropospheric degradation of non-aromatic volatile organic compounds, Atmos. Chem. Phys., 3, 161–180, doi:10.5194/acp-3-161-2003, 2003.

Sillman, S.: The relation between ozone, NO_x and hydrocarbons in urban and polluted rural environments, Atmos. Environ., 33, 1821–1845, 1999.

Stevenson, D. S., Young, P. J., Naik, V., Lamarque, J.-F., Shindell, D. T., Voulgarakis, A., Skeie, R. B., Dalsoren, S. B., Myhre, G., Berntsen, T. K., Folberth, G. A., Rumbold, S. T., Collins, W. J., MacKenzie, I. A., Doherty, R. M., Zeng, G., van Noije, T. P. C., Strunk, A., Bergmann, D., Cameron-Smith, P., Plummer, D. A., Strode, S. A., Horowitz, L., Lee, Y. H., Szopa, S., Sudo, K., Nagashima, T., Josse, B., Cionni, I., Righi, M., Eyring, V., Conley, A., Bowman, K. W., Wild, O., and Archibald, A.: Tropospheric ozone changes, radiative forcing and attribution to emissions in the Atmospheric Chemistry and Climate Model Intercomparison Project (ACCMIP), Atmos. Chem. Phys., 13, 3063–3085, doi:10.5194/acp-13-3063-2013, 2013.

Stockwell, W. R., Middleton, P., Chang, J. S., and Tang, X.: The second generation regional acid deposition model chemical mechanism for regional air quality modeling, J. Geophys. Res., 95, 16343–16367, 1990.

Stockwell, W. R., Kirchner, F., Kuhn, M., and Seefeld, S.: A new mechanism for regional atmospheric chemistry modeling, J. Geophys. Res.-Atmos., 102, 25847–25879, 1997.

Watson, L. A., Shallcross, D. E., Utembe, S. R., and Jenkin, M. E.: A Common Representative Intermediates (CRI) mechanism for VOC degradation. Part 2: Gas phase mechanism reduction, Atmos. Environ., 42, 7196–7204, 2008.

Yarwood, G., Rao, S., Yocke, M., and Whitten, G. Z.: Updates to the Carbon Bond Chemical Mechanism: CB05, Tech. rep., US Environmental Protection Agency, Novato, California, USA, 2005.

Supplement of Atmos. Chem. Phys., 15, 8795–8808, 2015
http://www.atmos-chem-phys.net/15/8795/2015/
doi:10.5194/acp-15-8795-2015-supplement

Atmospheric Chemistry and Physics Open Access

Supplement of

A comparison of chemical mechanisms using tagged ozone production potential (TOPP) analysis

J. Coates and T. M. Butler

Correspondence to: J. Coates (jane.coates@iass-potsdam.de)

S1 Introduction

This is the supplementary material to the research paper "A Comparison of Chemical Mechanisms using Tagged Ozone Production Potential (TOPP) Analysis" and provides further information about the methodology as well as additional analysis.

S2 Mechanism Setup

All chemical mechanisms were adapted from their original format into the modularised KPP (Damian et al., 2002) format for use in the MECCA boxmodel (Sander et al., 2005) as modified by (Butler et al., 2011).

The MCM v3.2 (Jenkin et al., 1997, 2003; Saunders et al., 2003; Bloss et al., 2005; Rickard et al., 2015) is the reference mechanism and its approach to dry deposition, photolysis and peroxy radical–peroxy radical reactions were applied to all mechanisms.

S2.1 Photolysis

Photolysis was parameterised as a function of the solar zenith angle following the MCM approach (Saunders et al., 2003). Species from reduced mechanisms with a direct counterpart in the MCM v3.2 were assigned the corresponding MCM v3.2 photolysis rate parameter. Otherwise, the recommended rate parameter in the mechanism determined the appropriate MCM v3.2 photolysis rate parameter. In some cases, the MCM v3.2 photolysis rate parameter closest in magnitude to that specified by the mechanism was used. For example, the organic nitrate species ONIT in RACM2 has a photolysis rate parameter of 1.96×10^{-6} s^{-1} that was compared to the MCM v3.2 organic nitrate photolysis rate parameters (J_{51} – J_{57}). The rate parameter J_{54} is the most similar in magnitude and was assigned as the ONIT photolysis rate parameter in RACM2.

Photolysis reactions of a species in reduced mechanisms were sometimes represented by more than one MCM v3.2 photolysis reaction. The product yields of the original mechanism reactions were preserved using combinations of the MCM v3.2 rate parameters. For example, glyoxal photolysis described by (R1) and (R2) in RADM2.

$$\mathrm{GLY} + \mathrm{h}\nu \longrightarrow 0.13\ \mathrm{HCHO} + 1.87\ \mathrm{CO} + 0.87\ \mathrm{H_2} \quad \text{(R1)}$$

$$\mathrm{GLY} + \mathrm{h}\nu \longrightarrow 0.45\ \mathrm{HCHO} + 1.55\ \mathrm{CO} + 0.8\ \mathrm{HO_2} + 0.15\ \mathrm{H_2} \quad \text{(R2)}$$

	Rate Parameter	MCM v3.2 Products and Yields
(R1)	0.87 J_{31}	1.74 CO + 0.87 H_2
	0.13 J_{32}	0.13 CO + 0.13 HCHO
	0.87 J_{31} + 0.13 J_{32}	1.87 CO + 0.13 HCHO + 0.87 H_2
(R2)	0.15 J_{31}	0.30 CO + 0.15 H_2
	0.45 J_{32}	0.45 CO + 0.45 HCHO
	0.4 J_{33}	0.80 CO + 0.80 HO_2
	0.15 J_{31} + 0.45 J_{32} + 0.4 J_{33}	1.55 CO + 0.45 HCHO + 0.80 HO_2 + 0.15 H_2

Table S1: Calculation of glyoxal MCM v3.2 photolysis rate parameters retaining RADM2 glyoxal photolysis product yields.

Mechanism	Reaction	Rate Constant
MCM v3.2	C2H5O2 = C2H5O	k*RO2*0.6 s^{-1}
	C2H5O2 = C2H5OH	k*RO2*0.2 s^{-1}
	C2H5O2 = CH3CHO	k*RO2*0.2 s^{-1}
MOZART-4	C2H5O2 + CH3O2 = 0.7 CH2O + 0.8 CH3CHO + HO2 + 0.3 CH3OH + 0.2 C2H5OH	2×10^{-13} cm^3 $molecules^{-1}$ s^{-1}
	C2H5O2 + C2H5O2 = 1.6 CH3CHO + 1.2 HO2 + 0.4 C2H5OH	6.8×10^{-14} cm^3 $molecules^{-1}$ s^{-1}
MOZART-4 modified	C2H5O2 = 0.8 CH3CHO + 0.6 HO2 + 0.2 C2H5OH	2×10^{-13}*RO2 s^{-1}

Table S2: Ethyl peroxy radical ($C_2H_5O_2$) self and cross organic peroxy reactions in MCM v3.2 and MOZART-4 including rate constants. $k = 2(6.6 \times 10^{-27} \exp(365/T))^{\frac{1}{2}}$ $molecules^{-1}$ s^{-1} and RO2 is the sum of all organic peroxy radical mixing ratios.

Whereas in the MCM v3.2, (R3), (R4) and (R5) are prescribed for glyoxal photolysis with the rates J_{31}, J_{32} and J_{33}.

$$\text{GLYOX} + h\nu \longrightarrow 2\ \text{CO} + 2\ \text{H}_2 \quad \text{(R3)}$$

$$\text{GLYOX} + h\nu \longrightarrow 2\ \text{CO} + 2\ \text{HO}_2 \quad \text{(R4)}$$

$$\text{GLYOX} + h\nu \longrightarrow \text{HCHO} + \text{CO} \quad \text{(R5)}$$

The product yields in (R1) were retained using a photolysis rate parameter of 0.87 J_{31} + 0.13 J_{32}, whilst for (R2) the rate 0.15 J_{31} + 0.45 J_{32} + 0.4 J_{33} was used. Table S1 illustrates the product yield calculations.

Reactants	**Products**	**Rate Constant**
MO2 + MO2	0.74 HO2 + 1.37 HCHO + 0.63 MOH	$9.4 \times 10^{-14} \exp(390/T)$ cm^3 molecules^{-1} s^{-1}
MO2	0.37 HO2 + 0.685 HCHO + 0.315 MOH	$9.4 \times 10^{-14} \exp(390/T)$*RO2 s^{-1}
ETHP + MO2	HO2 + 0.75 HCHO + 0.75 ACD + 0.25 MOH + 0.25 EOH	$1.18 \times 10^{-13} \exp(158/T)$ cm^3 molecules^{-1} s^{-1}
ETHP	0.63 HO2 + 0.065 HCHO + 0.75 ACD + 0.25 EOH	$1.18 \times 10^{-13} \exp(158/T)$*RO2 s^{-1}

Table S3: Dermination of ETHP pseudo-unimolecular reaction and rate constant in RACM2 including rate constants. RO2 is the sum of all organic peroxy radical mixing ratios.

S2.2 Organic Peroxy Radical Self and Cross Reactions

Reactions of organic peroxy radicals (RO_2) with other organic peroxy radicals are divided into self ($RO_2 + RO_2$) and cross (RO_2 + $R'O_2$) reactions. These reactions are typically represented in chemical mechanisms as bimolecular reactions which would cause ambiguities when implementing the tagging scheme. Namely, which tag to be used for the products of reactions between RO_2 reactants having different tags. The MCM v3.2 approach to self and cross RO_2 reactions (each RO_2 species reacts with the pool of all other RO_2 at a single uniform rate) is used to avoid such ambiguities. The MCM v3.2 approach represents RO_2–RO_2 reactions as a pseudo-unimolecular reaction whose rate constant includes a factor 'RO2' which is the sum of the mixing ratios of all organic peroxy radicals (Saunders et al., 2003).

The pseudo-unimolecular reaction products and their yields were determined by one of two methods. Firstly, by using the $RO_2 + RO_2$ reaction and halving the product yields, demonstrated for the MOZART-4 treatment of the ethyl peroxy radical in Table S2. Alternatively, the $RO_2 + CH_3O_2$ reaction was used to determine the products due to CH_3O_2 and these products are then removed.

Table S3 demonstrates the steps determining the ETHP pseudo-unimolecular reaction in RACM2. First the products due to MO2 (CH_3O_2 in RACM2) are determined as outlined previously using the MO2 + MO2 reaction. The MO2 product yields are subtracted from the ETHP + MO2 reaction. Any products having a negative yield are not included in the

final pseudo-unimolecular reaction.

The methyl acyl peroxy radical ($CH_3C(O)O_2$) was the exception to the above approach. Although most mechanisms include a $CH_3C(O)O_2 + CH_3C(O)O_2$ reaction, the $CH_3C(O)O_2$ pseudo-unimolecular reaction was derived by subtracting the CH_3O_2 product yields from the $CH_3C(O)O_2 + CH_3O_2$ reaction. This approach was used as the $CH_3C(O)O_2 + CH_3O_2$ reaction is the most significant reaction for $CH_3C(O)O_2$.

The rate constant for each pseudo-unimolecular reaction was taken as that of the $RO_2 + CH_3O_2$ reaction multiplied by an 'RO2' factor, which is the sum of the mixing ratios of all organic peroxy radicals. The $RO_2 + CH_3O_2$ rate constant was chosen as this is the most likely reaction to occur.

Model runs using the original and modified approach to the RO_2–RO_2 reactions for each mechanism were performed. The resulting O_3 concentration time series were compared and shown in Figure S1.

S2.3 Dry Deposition

Dry deposition velocities for individual chemical species are taken from the MCM v3.2. The MCM v3.2 dry deposition velocities of the same chemical functional group were used for mechanism species without direct MCM v3.2 analogues. For example, the dry deposition velocity of PAN-like species in all mechanisms was equivalent to that of the PAN species in the MCM v3.2.

S2.4 Negative Product Yield Treatment

Some mechanisms include reactions where products have a negative yield. These reactions were re-written including an operator species with a positive yield as the analysis tools used in this study do not allow negative product yields. The operator species acts as a sink for the original product by immediately reacting with the original product generating a 'NULL' product.

For example, in RADM2 the OH + CSL (cresol) reaction has negative OH yield in (R6) (Stockwell et al., 1990).

$$\text{CSL} + \text{OH} \longrightarrow 0.1\ \text{HO}_2 + 0.9\ \text{XO}_2 + 0.9\ \text{TCO}_3 - 0.9\ \text{OH} \quad \text{(R6)}$$

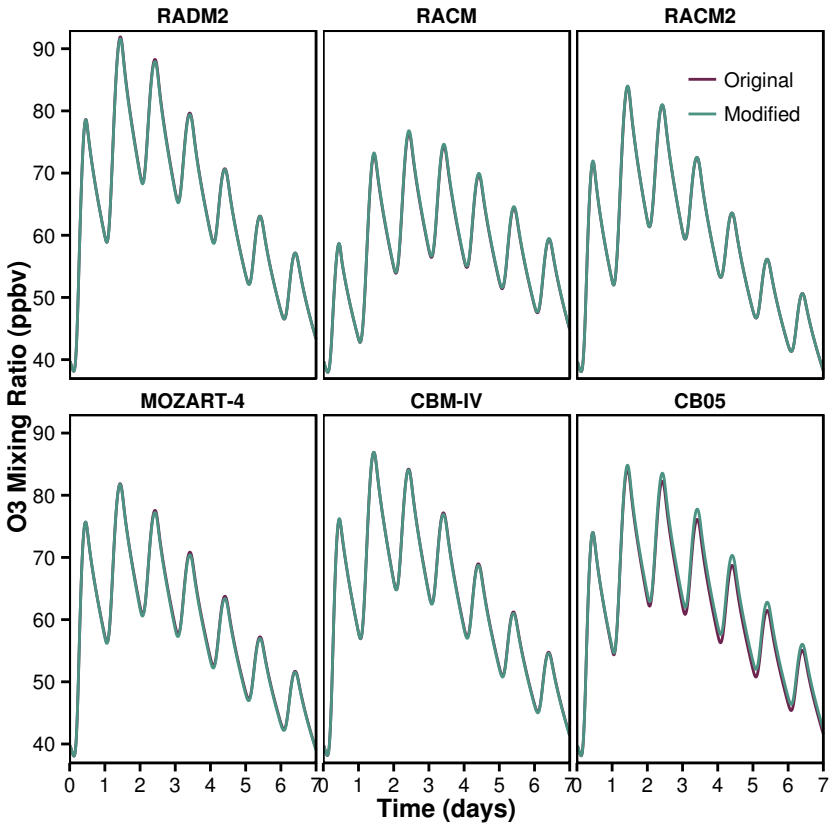

Figure S1: O_3 mixing ratio time series for each reduced mechanism using the original and modified approach to RO_2–RO_2 reactions

The negative OH yield was adapted to a positive operator (OHOP) yield in (R7). OHOP then reacts immediately with OH giving a 'NULL' product with a rate constant of 8.0×10^{-11} cm^3 s^{-1} (R8). Thus preserving the OH yields from (R6) in RADM2.

$$\text{CSL} + \text{OH} \longrightarrow 0.1\ \text{HO}_2 + 0.9\ \text{XO}_2 + 0.9\ \text{TCO}_3 + 0.9\ \text{OHOP} \quad \text{(R7)}$$

$$\text{OHOP} + \text{OH} \longrightarrow \text{NULL} \quad \text{(R8)}$$

S3 Mapping Emitted NMVOC to Mechanism Species

The emitted NMVOC are typical of Los Angeles as described in Baker et al. (2008). The MCM v3.2, v3.1 (Jenkin et al., 1997; Saunders et al., 2003; Jenkin et al., 2003) and CRI v2 (Jenkin et al., 2008) explicitly represent all of these NMVOC.

The representation of NMVOC in all other mechanisms required mapping the individual NMVOC to specific mechanism species. This mapping followed the recommendations on

the literature of the mechanism; Table S4 describes the mechanism species used for mapping the initial NMVOC. Table 2 of the main article shows the final mapping of each NMVOC to each mechanism species.

S4 Treatment of 2-methylpropene Degradation

Figure 4 of the main article shows the first day TOPP values of the VOC obtained in each reduced mechanism compared to the MCM v3.2. The first day TOPP values of 2-methylpropene in RACM, RACM2, MOZART-4, CBM-IV and CB05 signify differences in its degradation to the MCM v3.2.

The variation between RACM, RACM2 and MCM v3.2 arises from differences in the ozonolysis rate constant of 2-methylpropene. This rate constant is an order of magnitude faster in RACM and RACM2 than in MCM v3.2 as the RACM, RACM2 rate constant is a weighted mean of the ozonolysis rate constants of each VOC represented as OLI (Stockwell et al., 1997; Goliff et al., 2013). The faster rate constant promotes increased radical production leading to more O_x in RACM and RACM2 than the MCM v3.2.

2-methylpropene is represented as BIGENE in MOZART-4. The degradation of BIGENE produces CH_3CHO through the reaction between NO and the 2-methylpropene peroxy radical, whereas no CH_3CHO is produced during 2-methylpropene degradation in the MCM v3.2. CH_3CHO initiates a degradation chain producing O_x involving CH_3CO_3 and CH_3O_2 leading to more O_x in MOZART-4 than MCM v3.2.

CBM-IV and CB05 represent 2-methylpropene as a combination of aldehydes and PAR, the C−C bond (Gery et al., 1989; Yarwood et al., 2005). This representation of 2-methylpropene does not produce the 2-methylpropene peroxy radical, whose reaction with NO is the main source of O_x production in all other mechanisms.

Mechanism	Species	Description
MOZART-4 (Emmons et al., 2010)	C2H6	Ethane
	C3H8	Propane
	BIGALK	Lumped alkanes C >3
	C2H4	Ethene
	C3H6	Propene
	BIGENE	Lumped alkenes C >3
	ISOP	Isoprene
	TOLUENE	Lumped aromatics
RADM2 (Stockwell et al., 1990)	ETH	Ethane
	HC3	OH rate constant (298, 1 atm) between 2.7×10^{-13} and 3.4×10^{-12}
	HC5	OH rate constant (298, 1 atm) between 3.4×10^{-12} and 6.8×10^{-12}
	HC8	OH rate constant (298, 1 atm) greater than 6.8×10^{-12}
	OL2	Ethene
	OLT	Terminal Alkenes
	OLI	Internal Alkenes
	ISO	Isoprene
	TOL	Toluene and less reactive aromatics
	XYL	Xylene and more reactive aromatics
RACM (Stockwell et al., 1997)	ETH	Ethane
	HC3	OH rate constant (298 K, 1 atm) less than 3.4×10^{-12} cm^3 s^{-1}
	HC5	OH rate constant (298 K, 1 atm) between 3.4×10^{-12} and 6.8×10^{-12} cm^3 s^{-1}
	HC8	OH rate constant (298 K, 1 atm) greater than 6.8×10^{-12}
	ETE	Ethene
	OLT	Terminal alkenes
	OLI	Internal alkenes
	ISO	Isoprene
	TOL	Toluene and less reactive aromatics
	XYL	Xylene and more reactive aromatics
RACM2 (Goliff et al., 2013)	ETH	Ethane
	HC3	OH rate constant (298 K, 1 atm) less than 3.4×10^{-12} cm^3 s^{-1}
	HC5	OH rate constant (298 K, 1 atm) between 3.4×10^{-12} and 6.8×10^{-12} cm^3 s^{-1}
	HC8	OH rate constant (298 K, 1 atm) greater than 6.8×10^{-12} cm^3 s^{-1}
	ETE	Ethene
	OLT	Terminal alkenes
	OLI	Internal alkenes
	ISO	Isoprene
	BEN	Benzene
	TOL	Toluene and less reactive aromatics
	XYM	m-Xylene
	XYO	o-Xylene
	XYP	p-Xylene
CBM-IV (Gery et al., 1989)	PAR	Paraffin carbon bond C−C
	ETH	Ethene
	OLE	Olefinic carbon bond C=C
	ALD2	High molecular weight aldehydes
	ISOP	Isoprene
	TOL	Toluene
	XYL	Xylene
	FORM	Formaldehyde
CB05 (Yarwood et al., 2005)	ETHA	Ethane
	PAR	Paraffin carbon bond C−C
	OLE	Terminal olefin carbon bond R−C=C
	FORM	Formaldehyde
	ISOP	Isoprene
	TOL	Toluene and other monoalkyl aromatics
	XYL	Xylene and other polyalkyl aromatics

Table S4: Description of primary mechanism species used for mapping emitted NMVOCs.

References

Angela K. Baker, Andreas J. Beyersdorf, Lambert A. Doezema, Aaron Katzenstein, Simone Meinardi, Isobel J. Simpson, Donald R. Blake, and F. Sherwood Rowland. Measurements of nonmethane hydrocarbons in 28 United States cities. *Atmospheric Environment*, 42: 170–182, 2008.

C. Bloss, V. Wagner, M. E. Jenkin, R. Vollamer, W. J. Bloss, J. D. Lee, D. E. Heard, K. Wirtz, M. Martin-Reviejo, G. Rea, J. C. Wenger, and M. J. Pilling. Development of a detailed chemical mechanism (MCMv3.1) for the atmospheric oxidation of aromatic hydrocarbons. *Atmospheric Chemistry and Physics*, 5:641–664, 2005.

T. M. Butler, M. G. Lawrence, D. Taraborrelli, and J. Lelieveld. Multi-day ozone production potential of volatile organic compounds calculated with a tagging approach. *Atmospheric Environment*, 45(24):4082–4090, 2011.

V. Damian, A. Sandu, M. Damian, F. Potra, and G.R. Carmichael. The kinetic preprocessor KPP - A software environment for solving chemical kinetics. *Computers and Chemical Engineering*, 26(11):1567–1579, 2002.

L. K. Emmons, S. Walters, P. G. Hess, J.-F. Lamarque, G. G. Pfister, D. Fillmore, C. Granier, A. Guenther, D. Kinnison, T. Laepple, J. Orlando, X. Tie, G. Tyndall, C. Wiedinmyer, S. L. Baughcum, and S. Kloster. Description and evaluation of the Model for Ozone and Related chemical Tracers, version 4 (MOZART-4). *Geoscientific Model Development*, 3: 43–67, 2010.

Michael W. Gery, Gary Z. Whitten, James P. Killus, and Marcia C. Dodge. A photochemical kinetics mechanism for urban and regional scale computer modeling. *Journal of Geophysical Research*, 94(D10):12,925–12,956, 1989.

Wendy S. Goliff, William R. Stockwell, and Charlene V. Lawson. The regional atmospheric chemistry mechanism, version 2. *Atmospheric Environment*, 68:174–185, 2013.

M. E. Jenkin, S. M. Saunders, V. Wagner, and M. J. Pilling. Protocol for the development of the Master Chemical Mechanism, MCM v3 (Part B): Tropospheric degradation of aromatic volatile organic compounds. *Atmospheric Chemistry and Physics*, 3(1):181–193, 2003.

M. E. Jenkin, L. A. Watson, S. R. Utembe, and D. E. Shallcross. A Common Representative Intermediates (CRI) mechanism for VOC degradation. Part 1: Gas phase mechanism development. *Atmospheric Environment*, 42:7185–7195, 2008.

Michael E. Jenkin, Sandra M. Saunders, and Michael J. Pilling. The tropospheric degradation of volatile organic compounds: A protocol for mechanism development. *Atmospheric Environment*, 31(1):81–104, 1997.

Andrew Rickard, Jenny Young, and Stephen Pascoe. The Master Chemical Mechanism Version MCM v3.2. `http://mcm.leeds.ac.uk/MCMv3.2/`, 2015. [Online; accessed 25-March-2015].

R. Sander, A. Kerkweg, P. Jöckel, and J. Lelieveld. Technical Note: The new comprehensive atmospheric chemistry module MECCA. *Atmospheric Chemistry and Physics*, 5:445–450, 2005.

S. M. Saunders, M. E. Jenkin, R. G. Derwent, and M. J. Pilling. Protocol for the development of the Master Chemical Mechanism, MCM v3 (Part A): Tropospheric degradation of non-aromatic volatile organic compounds. *Atmospheric Chemistry and Physics*, 3(1): 161–180, 2003.

William R. Stockwell, Paulete Middleton, Julius S. Chang, and Xiaoyan Tang. The Second Generation Regional Acid Deposition Model Chemical Mechanism for Regional Air Quality Modeling. *Journal of Geophysical Research*, 95(D10):16,343–16,367, 1990.

William R. Stockwell, Frank Kirchner, Michael Kuhn, and Stephan Seefeld. A new mechanism for regional atmospheric chemistry modeling. *Journal of Geophysical Research D: Atmospheres*, 102(22):25,847–25,879, 1997.

Greg Yarwood, Sunja Rao, Mark Yocke, and Gary Z. Whitten. Updates to the Carbon Bond Chemical Mechanism: CB05. Technical report, U. S Environmental Protection Agency, 2005.

Chapter 7

Paper 2: Variation of the NMVOC Speciation in the Solvent Sector and the Sensitivity of Modelled Tropospheric Ozone

Chapter 8

Paper 3: The Influence of Temperature on Ozone Production under varying NO_x Conditions – a modelling study

Chapter 9

Publication List

Appendix